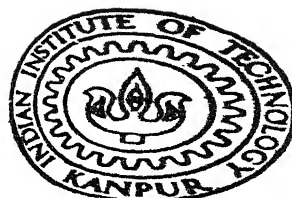


73

REDUCIBILITY OF IRON OXIDE IN METHANE - CONTAINING GASES

By
DINABANDHU GHOSH



DEPARTMENT OF METALLURGICAL ENGINEERING
INDIAN INSTITUTE OF TECHNOLOGY, KANPUR
JANUARY, 1981

REDUCIBILITY OF IRON OXIDE IN METHANE - CONTAINING GASES

A Thesis Submitted
in Partial Fulfilment of the Requirements
for the Degree of
MASTER OF TECHNOLOGY

By
DINABANDHU GHOSH

to the
DEPARTMENT OF METALLURGICAL ENGINEERING
IAN INSTITUTE OF TECHNOLOGY, KANPUR
JANUARY, 1981

L.I.T. PAMPUR
CENTRAL LIBRARY

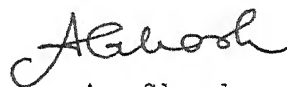
65988

16 MAY 1981

ME-1981-M-GHO-RED

C E R T I F I C A T E

Certified that this work on "Reducibility of Iron Oxide in Methane- containing Gases" has been carried out under my supervision and that it has not been submitted elsewhere for a degree.



A. Ghosh
Professor
Department of Metallurgical Engg.
Indian Institute of Technology
Kannur- 208016
U. P.

A C K N O W L E D G E M E N T

I take this opportunity to express my appreciation to Professor A. Ghosh who has guided and inspired me throughout the course of this investigation.

I am grateful to the Direct Reduction Process Development Division (DRPDD), Research and Development Centre, Steel Authority of India Limited, Ranchi for sponsoring this project, actively participating in formulating it, and deputing Mr. A.K. Roy from time to time to actively render his valuable help in this investigation. Discussions with Mr. Dixit, Dr. Thakur and their colleagues in DRPDD during the course of this investigation are greatly appreciated.

It is a pleasure to acknowledge the help rendered by Mr. S.C. Bachar who worked as a research assistant in this project for sometime and contributed a good deal especially during the experimental program. Thanks are also due to Mr. Sharma for active help in fabrication and other miscellaneous matters, Miss. Rama Devi for carbon determination, Mr. D.P. Tripathi and other members of the Process Research Laboratory and Deptt. of Metallurgical Engg. Thanks are also due to the people of the Glass Blowing Shop for their prompt service, Dr. Kunzru for helpful discussions, Mr. B.D. Biswas for typing the manuscript, Mr. V.P. Gupta for tracing the figures.

C O N T E N T S

<u>CHAPTER</u>		<u>Page No.</u>
	LIST OF FIGURES	... vii - viii
	LIST OF TABLES	... ix
	NOTATION	... x
	ABSTRACT	... xi - xii
I	INTRODUCTION	... 1 - 7
I.1	Scope of the work	... 3 - 4
I.2	Literature review	... 4 - 7
I.2.1	Earlier investigations on reduction of ferric oxide by hydrocarbons	... 4 - 6
I.2.2	Investigations on pyrolysis of methane	... 6 - 7
II	EXPERIMENTAL	... 8 - 25
II.1	Preparation of pure ferric oxide pellets	... 8 - 10
II.1.1	Preparation of porous pellets	... 8
II.1.2	Preparation of dense pellets	... 9 - 10
II.1.3	Measurement of porosities of pellets..	10
II.2	Experimental set-up to determine fractional reduction of a single pellet as a function of time	... 11-120
II.2.1	Methane generation and storage	... 11- 14
II.2.2	Gas train	... 14- 17
II.2.3	Thermogravimetric set-up	... 17- 20
II.3	Auxiliary measurements	... 20- 24
II.3.1	Analysis of exit gas by gas chromatograph	... 20- 21
II.3.2	Determination of carbon deposited on pellet and apparatus	... 21- 24

II.3.2.1	Gravimetric method	...	22 - 23
II.3.2.2	Volumetric method	...	23
II.3.3	Measurement of variation of temperature at the pellet centre	...	23 - 24
II.4	Experimental procedure	...	24 - 25
III	RESULTS	...	26 - 42
III.1	Presentation of results	...	26 - 29
III.2	Accuracy of measurements	...	29 - 38
III.3	Reproducibility and reliability of measurements	...	39
IV	DISCUSSION OF RESULTS	...	43 - 76
IV.1	Decomposition of methane	...	43 - 46
IV.2	Reduction of iron oxide - overall considerations	...	46 - 55
IV.3	Analysis of steady state region	...	55 - 62
IV.3.1	Dependence of rate on p_{H_2}	...	55 - 56
IV.3.2	Temperature dependence of reduction rate	...	56 - 62
IV.3.2.1	Consideration of overall reaction	...	56 - 60
IV.3.2.2	Consideration of reduction reaction	...	60 - 62
IV.4	Nature of F vs. t curves	...	63
IV.5	Carbon deposition on pellets..	...	63
IV.6	Change of temperature inside pellet during reduction	...	64 - 65
IV.7	Volume changes in pellets upon reduction	...	65
IV.8	Comparison of reduction of dense and porous pellets	...	69

II.3.2.1	Gravimetric method	...	22 - 23
II.3.2.2	Volumetric method	...	23
II.3.3	Measurement of variation of temperature at the pellet centre	...	23 - 24
II.4	Experimental procedure	...	24 - 25
III	RESULTS	...	26 - 42
III.1	Presentation of results	...	26 - 29
III.2	Accuracy of measurements	...	29 - 38
III.3	Reproducibility and reliability of measurements	...	39
IV	DISCUSSION OF RESULTS	...	43 - 76
IV.1	Decomposition of methane	...	43 - 46
IV.2	Reduction of iron oxide - overall considerations	...	46 - 55
IV.3	Analysis of steady state region	...	55 - 62
IV.3.1	Dependence of rate on p_{H_2}	...	55 - 56
IV.3.2	Temperature dependence of reduction rate	...	56 - 62
IV.3.2.1	Consideration of overall reaction	...	56 - 60
IV.3.2.2	Consideration of reduction reaction	...	60 - 62
IV.4	Nature of F vs. t curves	...	63
IV.5	Carbon deposition on pellets	...	63
IV.6	Change of temperature inside pellet during reduction	...	64 - 65
IV.7	Volume changes in pellets upon reduction	...	65
IV.8	Comparison of reduction of dense and porous pellets	...	69

Page No.

IV.9	Comparison of reduction of big and normal virus pellets...	69
IV.10	Rate controlling step for oxide reduction ...	69 - 73
IV.11	Comparison with literature ...	74 - 76
V	SUMMARY AND CONCLUSIONS ...	77 - 79
VI	RECOMMENDATIONS FOR FURTHER WORK ...	80
	REFERENCES ...	81 - 82

LIST OF FIGURESPage No.

II.1	Set-up for methane generation and storage	...	12
II.2	Lay-out of gas train	...	16
II.3	Thermogravimetric set-up	...	18
III.1	Effect of time and temperature on fractional reduction with methane at low flow rate	...	30
III.2	Effect of time and temperature on fractional reduction with methane at high flow rate	...	31
III.3	Variation of mole fraction of methane in exit gas with time at different temperatures	...	32
III.4	Variation of mole fraction of hydrogen in exit gas with time at different temperatures	...	33
III.5	Carbon deposition on pellets at different temperatures	...	34
III.6	Typical spring calibration curve...	...	35
III.7	Chromatographic traces	...	37
III.8	Fractional reduction vs. time plots for reduction with hydrogen at 800°C	...	40
III.9	Reproducibility of F vs. t curves for reduction with methane at high flow rate	...	41
III.10	Reproducibility of F vs. t curves for reduction with methane at low flow rate	...	42

Page No.

IV.1	Effect of time and different reducing gases on fractional reduction	...	47
IV.2	Effect of time and gas flow rate on fractional reduction	...	50
IV.3	Comparison of (r_{H_2O}/r_{H_2}) Actual with (r_{H_2O}/r_{H_2}) Equilibrium at different temperature	...	54
IV.4	Effect of partial pressure of hydrogen in exit gas on rate of oxygen removal	...	57
IV.5	Arrhenius plot for reduction at low flow rate	...	58
IV.6	Arrhenius plot for reduction at high flow rate	...	59
IV.7	$\log k_1$ vs. $\frac{1}{T}$ plot at high flow rate	...	62
IV.8	\dot{n}_O vs. F plot for different size and porosity at low gas flow rate..		67
IV.9	\dot{n}_O vs. F plot for different size and porosity at high gas flow rate.		68
IV.10	Arrhenius-type plot for methane decomposition in blank experiments.		75

LIST OF TABLES

		<u>Page No.</u>
III.1	Summary Table	... 27
IV.1	Comparison of (p_{H_2O}/p_{H_2}) actual with (p_{H_2O}/p_{H_2}) equilibrium	... 53
IV.2	Calculations of k_1 at different temperatures	... 61
IV.3	Size changes in pellet upon reduction	... 66
IV.4	Variation of x with temperature	... 74

N O T A T I O N

C_{H_2}	= Concentration of hydrogen, gm.mole/cc.
C_{H_2O}	= Concentration of moisture, gm.mole/cc.
d_o	= Original diameter of pellet, cm.
d_r	= Diameter of reduced pellet, cm.
F	= Fractional reduction of pellet, dimensionless.
F_{max}	= Maximum fractional reduction of pellet, dimensionless.
k_1, k'_1	= Rate constants, cc/sec.
K_e	= Equilibrium constant, dimensionless.
M_{Fe}	= Atomic weight of iron, dimensionless.
$M_{Fe_2O_3}$	= Molecular weight of ferric oxide, dimensionless.
\dot{n}_O	= Rate of oxygen removal from pellet, gm. atom/sec.
P_T	= Total pressure, atmosphere.
p	= Partial pressure of gas component, atmosphere.
T	= Temperature, $^{\circ}K$.
t	= Time, sec.
$t_{0.5}$	= Time for $F = 0.5$, sec.
\dot{V}	= Volumetric flow rate of gas component, cc(STP)/sec.
W	= Weight of pellet, gm.
\dot{W}_O	= Rate of oxygen removal from pellet, gm./sec.
X	= Mole fraction of gas component, dimensionless.
x	= Fraction methane decomposed, dimensionless.
Greek Letter :	
ϵ	= Fractional porosity of pellet, dimensionless.

A B S T R A C T

Solid state reduction of iron ores at low temperatures has attracted considerable interest in the recent past. Because of acute shortage of coking coal, severe scarcity along with its high price, and advantages in flexibility for choice of raw materials the trend towards this Direct Reduction route is increasing steadily.

The provocation behind this investigation is the reported success of the modified Rotary Kiln process which employs an underbed injection of hydrocarbon in the usual Rotary Kiln process. Present investigation used methane as reducing agent for the reduction of pure iron oxide spherical pellet. Sometimes, methane-hydrogen mixture of hydrogen alone has been used for comparative study. Experiments (Thermogravimetric) have been conducted with various temperatures, flow rates and porosities of pellets. Simultaneously exit gas analyses has been done in each experiment. Carbon deposited on the pellet and on the apparatus due to cracking of methane have also been measured. Moreover, change of pellet temperature with time during reduction has been measured by embedding a thermocouple inside the pellet. The temperature range has been 800°C to 1025°C.

From the experimental results obtained so far it has been concluded that the cracking of methane on the inner surface of the Mullite tube which surrounds the pellet is controlling the overall rate to a great extent. Hydrogen gener-

ated through cracking of methane is the principal reducing agent. The process of reduction by hydrogen appears to be controlled by the rate of convective mass transfer in the gas boundary layer around the pellet. The apparent activation energies are 45.0 KJ/g.mole in the temperature range of 950°C - 1025°C and 15.3 KJ/g.mole in the temperature range of 875°C - 950°C. Carbon deposition increased rapidly with rise in temperature and varied between 0.02 to 3.15% of the weight of the reduced metal. It is not expected to block the pores significantly. The rates of reduction with methane were approximately 1/5th of those with pure hydrogen.

CHAPTER I

INTRODUCTION

Direct reduction of iron ores at low temperature has gained a considerable importance in recent years due to the fast depleting reserve of coking coal and the ever increasing demand for steel scrap. In the direct reduction of iron ores, the iron ores are reduced by a suitable reducing agent below the fusion temperature of iron. The various reducing agents employed are carbon, carbon monoxide, hydrogen or a mixture of CO and H₂. The reduction is carried out in various types of reactors, such as shaft furnaces, retorts, fluidized beds, rotary kilns etc. Of these, the rotary kiln process has the lowest initial investment and it can take care of low grade coal which is plenty in India. Hence, this process is found to be the most suitable under Indian context.

The conventional rotary kiln process uses only coal as reducing agent. The kiln is partially filled with the charge comprising ^{of} ore, coal and a desulphurising agent. The gases generated during reduction are burnt above the charge to meet the heat requirement of the process. Combustion is accomplished by supply of controlled amount of air at different parts of the kiln. The reduced material discharges from the kiln and is cooled before exposure to ambient conditions. It is crushed and magnetically separated from the char/gangue material.

A rotary kiln can be broadly divided into two zones — a preheating zone and a reduction zone. In the preheating zone the charge gets heated upto about 800°C accompanied by reduction of iron ore upto rustite phase while in the reduction zone reduction of rustite to metallic iron takes place. The main disadvantage of a rotary kiln is its low productivity. The productivity of a rotary kiln is around $0.2 \text{ ton of Fe/day.m}^3$ as compared to $2.0 \text{ tons of Fe/day.m}^3$ or more in blast furnace. Therefore, efforts should be made to increase the productivity of a rotary kiln. Considerable work has been done in this direction.

The latest innovations in this area are submerged air injection in the preheating zone and the underbed injection of a hydrocarbon (liquid or gaseous) in the reduction zone. It is claimed that the submerged air injection in the preheating zone reduces the length of the preheating zone so that for a given length of the kiln the reduction zone becomes longer, leading to possible lowering of operating temperature. The beneficial effects claimed due to underbed injection of hydrocarbons include shorter reduction times, lower operating temperatures, increased productivity, closer control over sponge composition with desired carbon contents over a wide range, absence of typical operational problems like ring formation etc. It is expected that the hydrocarbon decomposes partially inside the charge, generating active species of carbon and hydrogen which lead to significant improvement in reduction kinetics.

The Direct Reduction Process Development Division of Research and Development Center, Steel Authority of India Limited, Ranchi desired that some fundamental studies on the reduction of iron ore/oxide pellet in methane containing gases be conducted. The results of these studies may help them in knowing how the hydrocarbon injection in the reduction zone of the rotary kiln improves the kiln performance.

I.1 Scope of the Work

The scope of the work was tentatively drawn by mutual discussions and it is as follows :

To study the iron oxide-methane interaction at elevated temperatures, initially the approach would be to carry out experiments similar to those reported in literature, followed by new experiments and interpretation of data to the extent possible.

The program of the present investigation is as noted below :

- (i) Preparation of pure ferric oxide pellets of different sizes and porosities by hand rolling and sintering.
- (ii) Single pellet weight loss measurements by a thermogravimetric apparatus using H_2 , CH_4 , $H_2 + CH_4$ as reducing gases at the temperatures ranging from $800^\circ C$ to $1100^\circ C$.
- (iii) Gas purification and extensive analysis of reactant as well as product gases.

- (iv) Measurement of temperature changes in the pellet during reduction.
- (v) Analysis of the reduced product by a layerwise determination of metallic iron and carbon (free and combined).
- (vi) Identification of iron carbide in the product.
- (vii) A study of the microstructure of the reduced sample from the periphery to the core of the pellet.

I.2 Literature Review

I.2.1 Earlier investigations on reduction of ferric oxide by hydrocarbons :-

Investigations on reduction of iron ores have been carried out using mostly H_2 , CO, and gas mixture containing H_2 and CO. Very few investigations could be located when hydrocarbons have been employed directly for reduction. This is because hydrocarbons are first reformed into a gas mixture containing H_2 and CO, which is subsequently employed for reduction.

Mullett et al⁽¹⁾ showed that at temperatures below $930^\circ C$ consistently better reductions of prefluxed Consett sinter were obtained in a laboratory kiln using hydrogen - carbon dioxide - butane mixture, in which the hydrocarbon was reformed within the kiln, than when chemically equivalent hydrogen - carbon monoxide mixtures were used.

Nixon⁽²⁾ explained the favourable results of butane injection by the high reactivity of the 'nascent' carbon monoxide, carbon and hydrogen produced by the autocatalyzed reaction of hydrocarbon on the surface of the partly reduced ore particles⁽³⁾. After the initial burst of reaction, caused by the activated molecules or radicals of the reducing gases reacting at the surface of the partly reduced ore, the further influence of the hydrocarbon feedstock on the rate of reaction were predicted by the requirements of diffusion in the solid. The diffusion of gases are enhanced by micropores and macrocracks induced by the reaction of the hydrocarbon. Increased pore surface areas were observed by Nixon et al⁽⁴⁾.

Misra⁽⁵⁾ made a systematic study on the reduction of hematite with methane directly and compared with that of reduction with H_2 . It was seen that the rate of reduction with CH_4 was always less than that with H_2 . For the reduction of hematite with CH_4 , above 30 % reduction, apparent activation energy was found to be of the order of 46 KJ/gm.mole in the temperature range $900^\circ C - 1000^\circ C$ and 2.73 KJ/gm.mole in the temperature range $800^\circ C - 900^\circ C$. At about 15 % reduction, the apparent activation energy was of the order of 2.73 KJ/gm.mole. Studies were made on the rate of decomposition of methane on reduced iron, and an activation energy of the order of 63.84 KJ/gm.mole was found. From the theoretical calculations, the apparent activation energy for the diffusion of CH_4 in $CH_4 - H_2$ mixture was found to be of the order of 1.8 KJ/gm. mole.

The results of the above investigation were analyzed with the aid of different kinetic model and it was found that in the temperature range 900°C - 1000°C , the decomposition of methane to carbon and hydrogen was found to be the rate controlling step in the reduction of hematite with methane, whereas in the temperature range 800°C - 900°C , diffusion across the outside carbon layer was found to be the rate controlling step.

Thermodynamic calculations for the reduction of FeO with CH_4 showed that there is complete conversion of methane, and carbon is not present at equilibrium which proves methane to be an effective reducing agent for the reduction of iron ores.

1.2.2 Investigations on pyrolysis of methane :

The pyrolysis of methane was investigated by many workers. An excellent summary of earlier work is given by Egloff⁽⁶⁾. It is generally believed that the cracking takes place via free radical mechanism, Eisenberg and Bliss⁽⁷⁾ studied the pyrolysis of methane in a tubular reactor between 1100°C and 1200°C and showed conclusively that methane pyrolysis is not a first order reaction. Its rate may be described by a normal growth curve. They further showed that the rate is accelerated by ethane in the feed and inhibited by hydrogen. Syskov and Jelikhova⁽⁸⁾ studied the formation of coke from methane and suggested that coke mainly consists of high molecular weight aromatic hydrocarbons. Hirt and Palmer⁽⁹⁾ obtained an activation energy of 433KJ/mole

for homogeneous decomposition of methane into coke in flow reactor between 890°C and 1100°C. Albright and McConnell⁽¹⁰⁾ investigated the rate of coke formation in methane pyrolysis and found that the coking phenomenon was significantly affected by the material of construction of the pyrolysis tube. Although no quantitative expression for catalytic effect of metals and their oxides on pyrolysis of methane were not available, it is reported by Stanley and Nash⁽¹¹⁾ and Wheeler and Wood⁽¹²⁾ that metals like iron, nickel, cobalt, copper, platinum and palladium tend to promote the total decomposition of methane to carbon and hydrogen.

CHAPTER II

E X P E R I M E N T A L

Experimental program may be conveniently discussed under the following heads :

Preparation of pure ferric oxide pellets
Experimental set-up to determine fractional reduction of single pellet as a function of time
Auxiliary measurements
Experimental procedure

II.1 Preparation of Pure Ferric Oxide Pellets

II.1.1 Preparation of porous pellets :

Chemically pure (99.7%) commercial ferric oxide powder (Fischer Scientific Company) was sieved and the -200 mesh fraction was pelletised by moistening, hand-rolling and drying in oven at 110°C for 12 hours. These green spherical pellets were kept on an zirconia boat and introduced into a horizontal furnace with silicon carbide rods as heating elements. A heating rate of approximately 200°C per hour was maintained. An atmosphere of oxygen was kept in the furnace tube throughout the heating and cooling cycle. After a few trials, the temperature and time of sintering chosen to 1000°C and 3 hours respectively to obtain approximately 30% porous pellets.

II.1.2 Preparation of dense pellets :

For preparation of dense pellets it was felt that finer particle size of ferric oxide is required. The method of preparation followed was that given by Vogel⁽¹³⁾. A.R. grade ferrous ammonium sulphate was used as the starting material. A saturated solution of it was made with distilled water. This solution was heated to 70°C - 80°C and then concentrated nitric acid was added dropwise into it to oxidise the ferrous ions to ferric ions, the completion of which was indicated by a clear yellow colour of the solution. The resulting solution was boiled for few minutes to remove brown coloured gases likely to be oxides of nitrogen, and then allowed to cool down to 60°C - 70°C. Through this warm solution, ammonia gas was passed with stirring till precipitation of ferric hydroxide was complete. The ammonia gas was prepared in the laboratory by allowing concentrated ammonium hydroxide solution to react with solid sodium hydroxide. This method of precipitation was adopted to avoid possible contamination of ferric hydroxide with silica, tar etc. which would have resulted because of direct addition of ammonium hydroxide solution. The precipitate was then washed with hot distilled water repeatedly until complete removal of the adsorbed ammonia was accomplished. The washings were tested for ammonia by litmus paper. For a number of occasions, ammonium nitrate solution has been used along with hot distilled water for washing purpose. The precipitate was

then filtered and dried in oven at a temperature of 110°C for 8 hours. Ferric oxide was obtained from this ferric hydroxide precipitate by calcination at 700°C in oxygen atmosphere. The resulting ferric oxide was then ground by steel balls with adequate amount of water for 45 minutes. The fine particles of ferric oxide were then filtered and allowed to dry at room temperature. The pellets were prepared out of it by hand-rolling with the necessary amount of water as binder followed by drying in oven at 110°C for 12 hours. These green spherical pellets then followed the same route as in case of porous pellet preparation. Only differences to be noted are little slower heating and cooling rate to avoid possible thermal cracks, and sintering temperature and time as 1375°C and 4 hours respectively to attain approximately 5% porosity.

II.1.3 Measurement of porosities of pellets :

The weight of a pellet was measured accurately upto 0.0001 gm in a single pan semi-micro balance. The diameter of the pellet was measured by vernier slide callipers. Since the pellets were not exactly spherical, the diameter was measured along several directions and the average was accepted. From this average diameter, pellet volume was calculated. The ratio of the weight and the volume of the pellet gives the apparent density of the pellet. The fractional porosity was obtained from the following relation :

$$\text{Fractional porosity} = \frac{\text{Theoretical Density} - \text{Apparent Density}}{\text{Theoretical Density}}$$

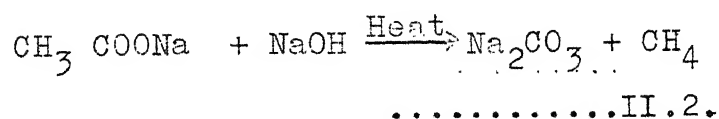
.....II.1

Theoretical density of ferric oxide was taken as 5.26 gm/cc. (14)

II.2 Experimental Set-up to Determine Fractional Reduction of a Single Pellet as a Function of Time

II.2.1 Methane generation and storage :

Fig. II.1 shows the set-up for generation and storage of methane. The reaction generating methane is as follows :



It is usually recommended to take sodium hydroxide in the form of soda lime. Soda lime was prepared by grinding and intimately mixing G.R. grade sodium hydroxide with calcium oxide in the 7 : 3 ratio. The resulting soda lime and A.R. grade sodium acetate were taken in 5 : 4 ratio, ground and mixed thoroughly. It had been established after a lot of trials that the optimum temperature of methane generation is around 400°C.

It was not possible to supply the methane generated according to reaction II.2 directly to the reduction chamber at a controlled flow rate. For this purpose, storage and pressurization of methane was necessary.

Fig. II.1 presents a sketch of the set-up for generation and storage of methane. The stoppered pyrex tube (No.2, Fig. II.1) contained the mixture of soda lime and sodium acetate. Rate of methane generation was slow at the beginning and then increased very rapidly. In order to prevent ejection of the neoprene stopper (No.3, Fig. II.1) by excess pressure,

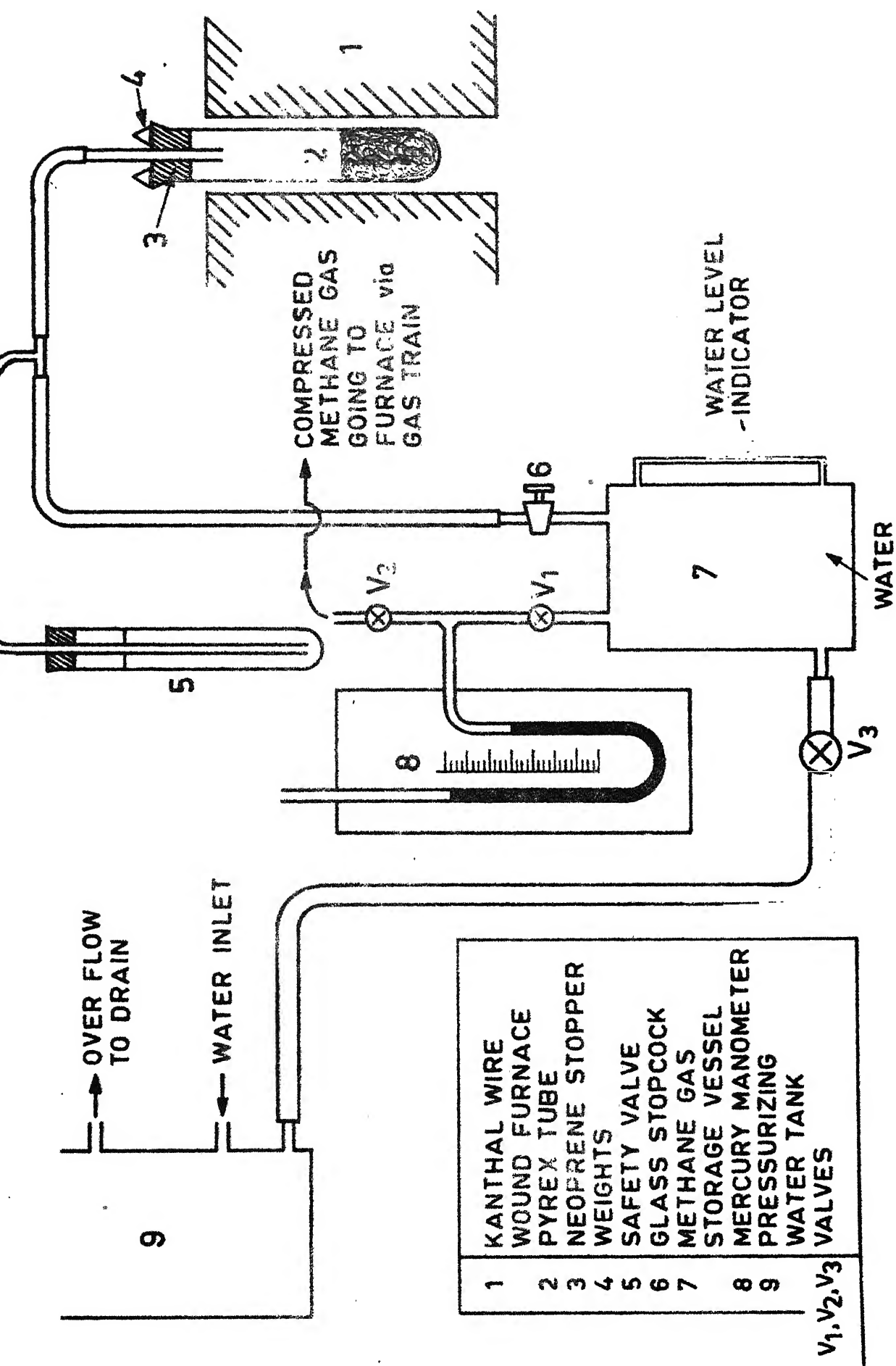


FIG. II.1 - SET-UP FOR GENERATION AND STORAGE OF METHANE GAS.

few a weights (No.4, Fig. II.1) were kept on the stopper. Also a safety valve (No.5, Fig. II.1) was installed in the by pass of methane line. The safety valve was nothing but an estimated amount of water head in a long glass tube dipped in a pool of water. V_1 , V_2 and V_3 were three valves which regulate the flow of fluids.

A mixture of 100 gms of sodium acetate and 80 gms of soda lime was taken as the starting material. This mixture after being properly ground and mixed was poured in a pyrex tube (No.2, Fig. II.1). In the mean time the storage vessel made of copper (No.7, Fig. II.1) was kept completely filled up with water upto V_1 and stop cock (No.6, Fig. II.1). The pyrex tube (No.2, Fig. II.1) was then gradually inserted in the furnace (No.1, Fig. II.1) which had already attained the required temperature (i.e. 400°C). Towards the start, the stopcock (No.6, Fig. II.1) was kept closed as lot of air used to come out along with methane. This impure methane used to be vented off through a bypass (No.5, Fig. II.1). After some time, when the gas generation rate became appreciable, stop cock (No.6, Fig. II.1) was opened and the valve V_3 was detached from the pressurizing water tank (No.9, Fig. II.1). The outlet of the water tank (No.9, Fig. II.1) which got isolated from V_3 was clamped so that water does not flow out of the tank. The valve V_2 was also kept closed but the valve V_1 was kept open to record the pressure of methane. A mercury manometer (No.8, Fig. II.1) was employed to indicate the pressure of methane. When rate of methane generation became too high or too

low as could be understood from both the manometer (No.8, Fig. II.1) and safety valve (No.5, Fig. II.1), the valve V_3 was manipulated to decrease or increase the exit water flow rate accordingly so that the methane generation and storage could take place at slightly above atmospheric pressure. After the completion of the methane generation, the stop-cock (No.6, Fig. II.1) was closed and the valve V_3 was again connected to the water tank (No.9, Fig. II.1). As a result the water rushes from the water tank (No.9, Fig. II.1) to the storage vessel (No.7, Fig. II.1) and compressed the methane gas. The compressed gas thus became ready for use.

During use of methane for reduction the pressure of the gas in the storage vessel (No.7, Fig. II.1) tends to drop. It was maintained almost constant because of in-flow of water from the over-head tank (No.9, Fig. II.1) into the storage vessel (No.7, Fig. II.1). The water level in the overhead tank (No.9, Fig. II.1) was maintained constant by ensuring over-flow all the time. Such precautions were needed in order to ensure a stable flowrate of methane into the thermogravimetric apparatus.

With 100 gms of sodium acetate and 80 gms. of soda line, methane generation was approximately 30 liters at STP. Pressurized methane attained approximately a pressure of 1.2 atm. The whole operation took about half an hour.

II.2.2 Gas Train :

A gas train was designed and fabricated to achieve the removal of impurities from the gases, the mixing of gases

in proper proportion whenever necessary, and the monitoring and controlling of gas flow rate. Fig. II.2 shows the layout of gas train and its basic components. Other than methane, hydrogen was sometimes used as reducing gas. Nitrogen or argon was employed for flusing^h the gas line before reduction. All these including oxygen which was used for carbon measurement were commercial cylinder gases. To remove oxygen from hydrogen, nitrogen and argon, these gases were passed through nicrome-wound copper gauze furnace heated at 400°C . After this, the purification train was applicable to oxygen gas also. This comprised of series of anhydrous calcium chloride columns to remove moisture followed by a soda lime column to entrap carbon dioxide. The purified gas then reached the mixer via a calibrated capillary flowmeter which registers the gas flow rate. A column of glass beads was used as the mixer.

Methane purification train contained only anhydrous calcium chloride column to absorb moisture, if any. The methane, free of moisture could be subjected to gas analysis whenever necessary by a three way stop cock arrangement. Gas analysis revealed only one percent of hydrogen and occasionally, a trace amount of air. One end of the stop cock led the methane gas to the mixer like other gas train via a calibrated flowmeter. However, mixing of two different gases became necessary on only one occasion where the mixture of hydrogen and methane was employed as reducing gas. From the mixture outlet the gas or gas mixture was fed directly to the inlet of the thermogravimetric set-up.

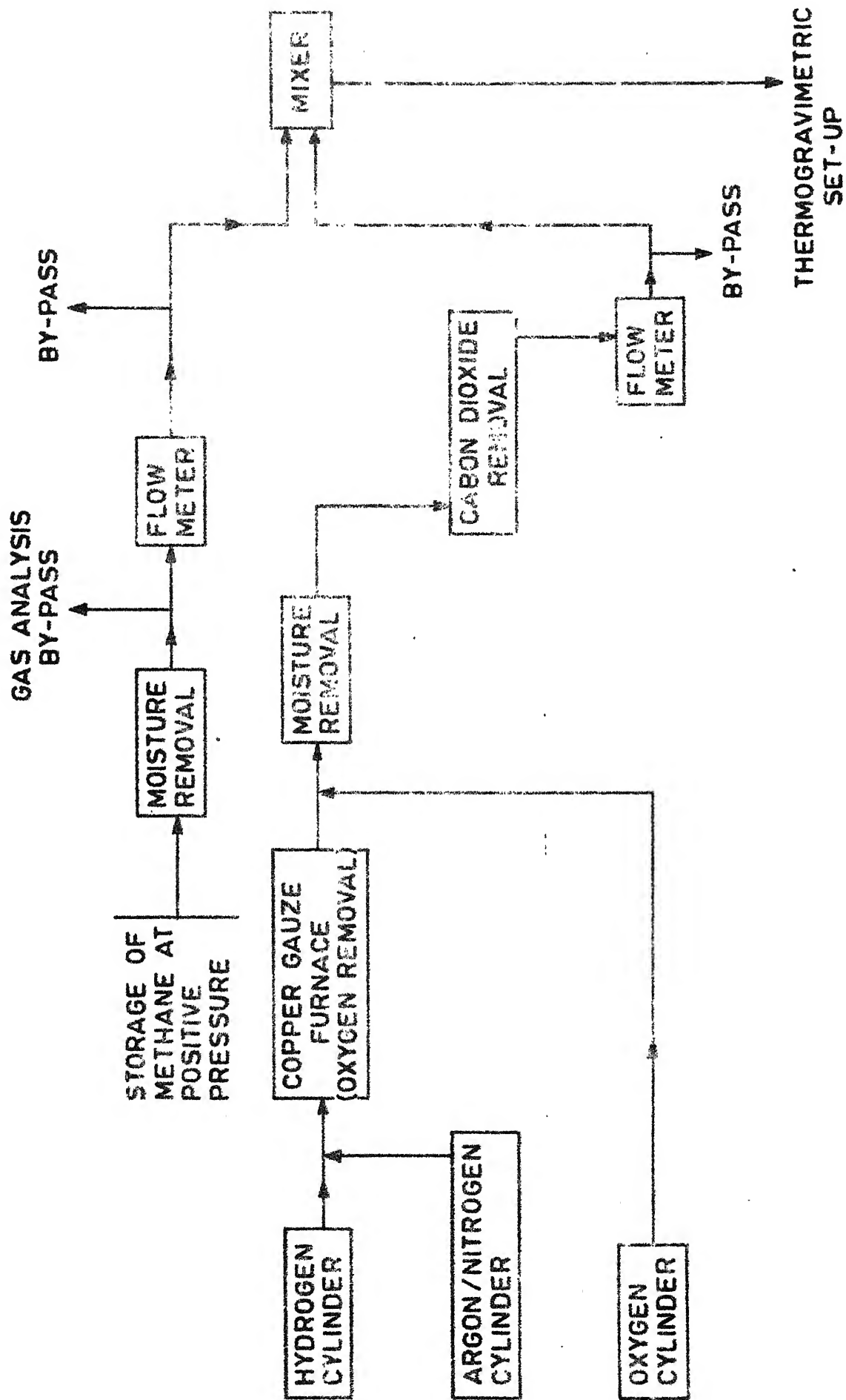
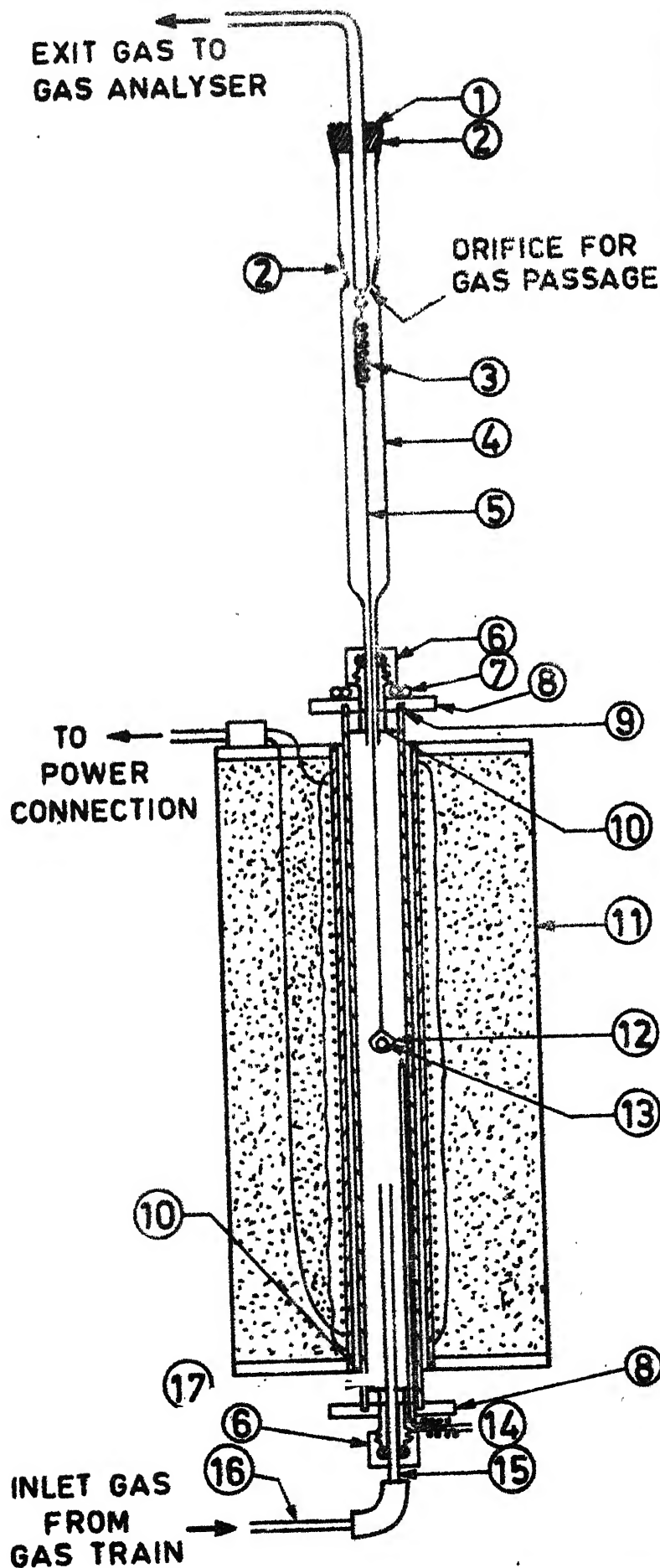


FIG. II.2 - LAY-OUT OF GAS TRAIN

Dibutyl phthalate liquid was used in both the flowmeters to monitor the flow rate. Extensive calibration of these flowmeters with different gases like H_2 , N_2 , CH_4 etc. was done with the help of a wet test meter (Toshniwal make) and corresponding calibration curves have been obtained.

II.2.3 Thermogravimetric set-up:

Fig. II.3 shows the sketch of the thermogravimetric set-up used for reduction experiments. The furnace assembly consisted of a Mullite tube of 5cm. I.D. mounted vertically inside a kenthel wound furnace. The uniform temperature zone at the centre of the furnace was approximately 5cm long. The pellet, contained in a platinum basket, was suspended from the last coil of the quartz spring with the help of a platinum wire. Both the ends of the Mullite tube were covered by brass heads carrying radiation shields. A glass tube was introduced through the hole at the top brass head. The elongated spring was contained in the upper portion of this glass tube. A ground glass joint covering the top of this tube provided the necessary hook to suspend the spring. Few orifices were provided near the top of the hook to allow smooth gas flow. The outlet gas line coming from the top of the ground glass joint via a neoprene stopper led to a bubbler followed by a 'Drierite' (anhydrous calcium sulphate) column to arrest the moisture, if any, with the exit gases. This was necessary because the exit gas samples were to be analysed by chromatograph which requires dry gas for proper operation. The gas sampling syringe collected



- | | |
|----|--------------------------------|
| 1 | NEOPRENE STOPPER |
| 2 | GROUND GLASS JOINT |
| 3 | QUARTZ SPRING |
| 4 | GLASS TUBE |
| 5 | PLATINUM WIRE |
| 6 | D-RING SEAL |
| 7 | COOLING COIL |
| 8 | BRASS HEAD |
| 9 | SILICONE SEALANT |
| 10 | RADIATION SHIELD |
| 11 | KANTHAL WIRE WOUND
FURNACE |
| 12 | PLATINUM BASKET |
| 13 | PELLET |
| 14 | CHROMEL-ALUMEL
THERMOCOUPLE |
| 15 | SILICA TUBE |
| 16 | GLASS TUBE |
| 17 | MULLITE TUBE |

FIG. II.3 - THERMOGRAVIMETRIC SET-UP.

the samples from the outlet of the 'Driemite' column. The bottom brass head had two openings. The bigger opening at the centre allowed insertion of a silica tube through which inlet gas coming from gas train flows to the reaction chamber. The tip of a chromel-alumel thermocouple was brought near ^{the} suspended pellet through the second opening to measure the temperature of the pellet. The joints of the glass tube with the top brass head and of the silica tube with the bottom one were made leak proof with the help of o-ring seals. Each brass head joint with the Mullite tube was made airtight by using silicone sealant. Similarly other joints with probable places of leakage were taken care of. Top brass head required cooling arrangement to protect o-ring seal which was done by circulating water through a copper coil affixed to the brass head by brazing.

The chromel-alumel thermocouple was attached to a ON-OFF temperature controller (Electromax) and a millivolt potentiometer (Leads and Northrup Co.) via a thermostat and a DPDT switch. Thermostat was used to achieve constant reference junction temperature. The thermocouple was normally connected to the controller. When temperature measurement by potentiometer was required, the connection was switched to the latter and disconnected from controller by operating the DPDT switch. Millivolt potentiometer was meant for precise measurement of temperature.

A cathetometer with a least count of 0.005cm, stationed a meter away from the furnace assembly perpendicular

to the direction of movement of the spring recorded the displacement of the spring. The cathetometer was focussed at the same point of the spring which was chosen also for calibration of the spring done earlier by calibrated standard weights.

II.3 Auxiliary Measurements

II.3.1 Analysis of exit gas by gas chromatograph :

As has been discussed in section II.2.3, the exit gas from the reduction chamber was collected from the outlet of a 'Drierite' column which absorbed the moisture of the gas, if any. A syringe (Top Syringemake) of 5cc. capacity was used for gas sampling. Usually, gas samples of 0.5cc. to 1cc. were drawn for each injection. The injection which immediately followed gas sampling was performed through the silicon septum to the adsorbing silica gel column of gas chromatograph which separates different gas components of the sample. The chromatograph was manufactured by the Chromatography and Instruments Company, Baroda (model no. AC1-TC). It had dual column, about 1.5 meter long and packed with silica gel. The presence and amount of different gas components is revealed from the different peaks recorded on the associated recorder (Omniscribe) chart-paper. Peaks appear as slightly distorted triangles whose areas are proportional to the volume of the corresponding gas component. The calibration of the chromatograph by pure gases like hydrogen, methane, carbon dioxide etc. was usually done on a regular basis before the exit gas analysis of the reduction

experiment started. Gas samples were taken at convenient times during the progress of the reduction. Peak areas were measured manually as integration facility in the recorder was not working.

The different operating conditions like the followings can be mentioned which may be useful :

- carrier gas used : nitrogen, hydrogen and argon depending on the requirement of the experiments.
- characteristic flow rate of carrier gas : 0.25cc (STP)/sec. for nitrogen and about 0.6cc (STP)/sec. for hydrogen.
- oven temperature : 108°C
- filament current : 100 mA
- attenuation : varied from 1 to 16 as and when required.
- full scale voltage of recorder output : 0.01 V.

II.3.2 Determination of carbon deposited on pellet and apparatus :

Carbon arising out of cracking of methane at reduction temperatures gets deposited on the apparatus as well as on the pellet. Attempts were made to determine the amount of carbon deposited by oxidation to carbon dioxide followed by gravimetric or volumetric measurement of carbon dioxide.

II.3.2.1 Gravimetric method :

In gravimetric method the carbon dioxide resulting from burning of carbon in oxygen at 900°C was passed through an 'Indicarb' (Fischer Scientific Co.) column via a U-tube filled with anhydrous calcium chloride to absorb moisture, if any. 'Indicarb' is an indicating carbon dioxide absorber. The ^{gas} coming out of the 'Indicarb' column was allowed to pass through a saturated solution of barium hydroxide followed by that of potassium hydroxide. The first one indicates the escape of any carbon dioxide from the 'Indicarb' column in the form of white barium carbonate precipitate while the second one is to resist any contamination of carbon dioxide from outside. Oxygen gas was passed for 35 - 45 minutes at a flow rate of 1.7cc (STP)/sec. The difference between final and initial weight of 'Indicarb' column, which is the amount of carbon dioxide absorbed, was measured precisely and carefully. Stoichiometrically, amount of carbon can be obtained from that carbon dioxide. First, the carbon deposited on the apparatus which includes everything other than the pellet was measured. Once carbon is removed from the apparatus, it could be used for measurement of carbon on the pellet by the same method.

The gravimetric method resulted a good conversion data (85%) with pure graphite. But unfortunately results did not appear reliable with carbon on pellet and apparatus for the reasons like tendency of 'Indicarb' to pick up moisture, consolidation of 'Indicarb' particles during progress of carbon

difficile absorption causing enormous pressure buildup inside the furnace followed by, leakage of carbon dioxide, occasional escape of carbon dioxide from the absorbing column as disclosed by white barium carbonate precipitate formation, inability to determine the carbon which penetrated inside the pellet etc.

II.3.2.2 Volumetric method :

The failure of the gravimetric method called for volumetric approach. In this case reduced pellet with deposited carbon was crushed and ground to very small pieces which were taken on a zirconia boat and introduced in the furnace at a temperature of about 1160°C . The standard apparatus (LECO, USA) which is used for determination of carbon in steel and cast iron by the combustion method was employed for this purpose. Purified oxygen gas, which was passed inside the furnace converts the carbon to carbon dioxide and iron to ferrous oxide rapidly. The latter gets fused at that temperature. The difference between the volume of outgoing oxygen and carbon dioxide combined and that of oxygen after carbon dioxide is absorbed by KOH solution gives the volume of carbon dioxide generated.

II.3.3 Measurement of variation of temperature at the pellet centre :

Variation of temperature with time at the pellet centre during usual reduction was measured. For this experiment, the thermocouple tip was embedded into the centre of the green pellet and then the pellet was sintered.

During reduction experiment this thermocouple recorded temperature of the pellet centre as a function of time while a separate thermocouple was inserted inside the furnace to control the temperature.

II.4 Experimental Procedure

The reduction furnace, the gas chromatograph, the methane generation furnace and the copper gauze furnace were gradually heated upto the desired temperatures. Methane was at first generated, stored, pressurized and thus kept ready for use. Gas chromatograph was then calibrated with different pure gases like H_2 , CH_4 , CO_2 etc. In the mean time, the gas train and the reduction chamber were flushed with argon (nitrogen, in a few experiments). The pellet with known weight, size etc. was put in the platinum basket. The assembly of calibrated spring, platinum wire and platinum basket was then slowly lowered into the reduction chamber to avoid thermal cracking of the pellet. The pellet was allowed to achieve thermal equilibrium. The temperature of the furnace was precisely measured by the millivolt potentiometer and fine adjustment in controller setting was done, if necessary, to achieve the desired temperature accurately. The desired flow rate of methane or/and hydrogen was established through a by-pass, before the gas was let into the reduction chamber. After the pellet had attained the desired temperature, the reducing gas was directed into the reduction furnace. The weight loss data were recorded at certain intervals. The zero time corresponded to that when the first change in weight was noticed in the form

of upward displacement of the spring. Exit gas samples were simultaneously drawn at certain intervals. The completion of reduction with methane was understood by the sudden downward movement of the spring. This was due to the result of carbon deposition on the pellet — the only reaction left after the oxygen in ferric oxide pellet is almost removed. However, methane was still passed for a few minutes to check that observation.

After complete reduction, the flow of reducing gas was stopped and the system was again flushed with inert gas to remove all other gases inside it and then only the reduced pellet was taken out slowly again to avoid thermal cracking.

CHAPTER III

R E S U L T S

Experimental results consist of

Fractional reduction vs. time data, and

Auxiliary measurements such as :

- analysis of exit gas during reduction as well as blank experiments
- carbon deposition on pellets
- size changes in pellets on reduction
- variation of temperature with time at the pellet centre during reduction as well as in blank experiment.

Experimental results can be conveniently discussed under the following heads :

Presentation of results

Accuracy of Measurements and

Reproducibility and Reliability of Measurements.

III.1 Presentation of Results

There were altogether 30 reliable experiments.

Table III.1 summerises the experimental conditions. It also shows the various measurements that were conducted and some experimentally determined characteristic data which do not depend on time.

Appendix A.I presents fractional reduction data at various times from the begining of experiment, gas analysis data and other observations separately for each experiment.

Few Notes About Table III.1

1. 'Carbon on pellet' should be little less than what shown in the table. This is due to the fact that CH_4 was passed for a while even after the reduction stopped in order to ensure the completion of reduction.
2. In 'gas analysis' N_2 symbolises that chromatographic gas analysis, which employed nitrogen as carrier gas, was done.
3. Experiments no.13 and 20 were deliberately stopped before the F_{max} values were attained.
4. In the experiments no.11,25 and 26 carbon deposited in the core of the pellet was separately measured.
5. Sign '-' means 'MEASUREMENTS NOT DONE'.

As table III.1 shows, the variations in experimental conditions may be summarized as :

Pellet Weight	:	0.875 gm	-	4.258 gm
Pellet Diameter	:	0.758 cm	-	1.266 cm
Fractional Porosity	:	0.000	-	0.346
Temperature	:	800°C	-	1025°C
Gas Flowrate	:	0.75	-	2.78 cc(STP)/ sec.for Methane
		7.65	-	18.24 cc(STP)/ sec.for Hydrogen
Flushing gas flow rate	:	8 cc(STP)/sec. (approx.)		

Though different parameters like pellet size, pellet porosity and methane flow rate have varied within a certain range as above, pellets with approximate diameters of 0.9cm. and 1.2cm. have been termed as normal size and big size pellets respectively. Similarly, pellets with approximate fractional porosity of 0.3 and 0.05 have been termed as porous and dense pellets respectively. Methane flowrate of about 0.75cc(STP)/sec. and 2.8cc(STP)/sec. have been taken as low and high flow rate respectively.

Fractional reduction vs. time data were not collected for all the experiments since some experiments were conducted for other purposes. For example, experiment nos. 24 and 25 were carried out under conditions identical to experiment no.21. But in experiment nos.24 and 25 the purpose was to determine the extent of carbon deposition on pellet at lower percentages of reduction.

Fractional reduction vs. time plots are shown in figs. III.1 and III.2. Variation of exit gas (i.e. methane and hydrogen) composition with time are presented in figs. III.3 and III.4. Quantities of carbon deposited expressed in gas as well as percentage of reduced pellet (i.e. iron) weight at different temperatures as shown in fig. III.5.

III.2 Accuracy of Measurements

- (a) The error in temperature measurement and control : $\pm 4^{\circ}\text{C}$ (approx.)
- (b) Inlet gas purity : Methane was 98.5% pure as analysed by gas chromatograph. Rest was hydrogen and sometimes, trace amount of air. Others were cylinder gases. There were hardly any other impurities in these gases because they were freed of oxygen, moisture and carbon dioxide in the gas train before introduction into the thermogravimetric apparatus.
- (c) Flow rate measurement: As mentioned in ch. II, the flow rates were measured by capillary flow meters which were extensively calibrated by the wet-test meter. The error involved was about $\pm 2\%$.
- (d) Weight loss measurement by spring : The spring calibration was quite reproducible. Fig. III.6 shows a typical calibration curve for the spring using calibrated standard weights. The sensitivity of the spring was estimated as one milligram.

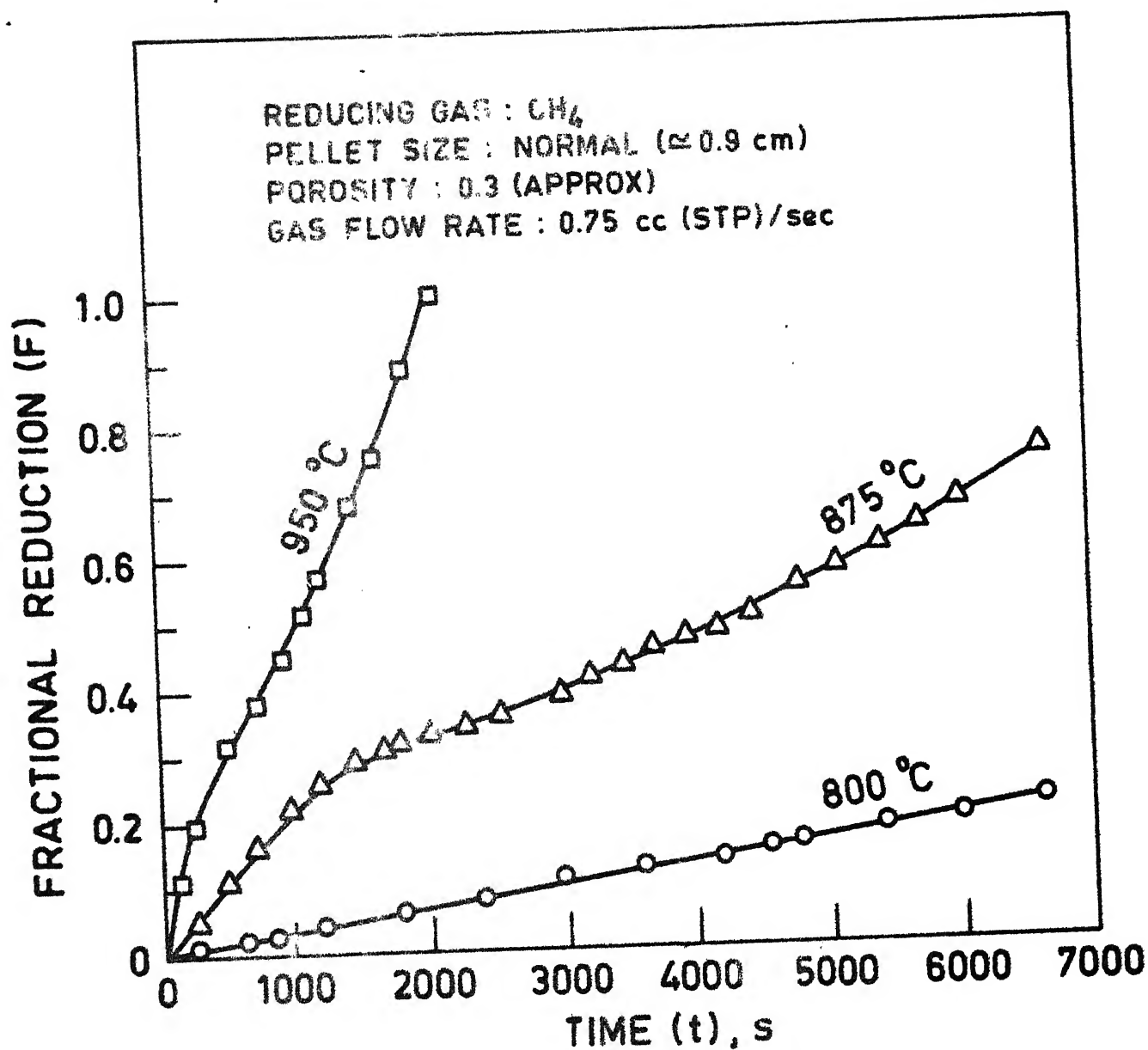


FIG. III.1 - EFFECT OF TIME AND TEMPERATURE ON FRACTIONAL REDUCTION WITH METHANE AT LOW FLOW RATE.

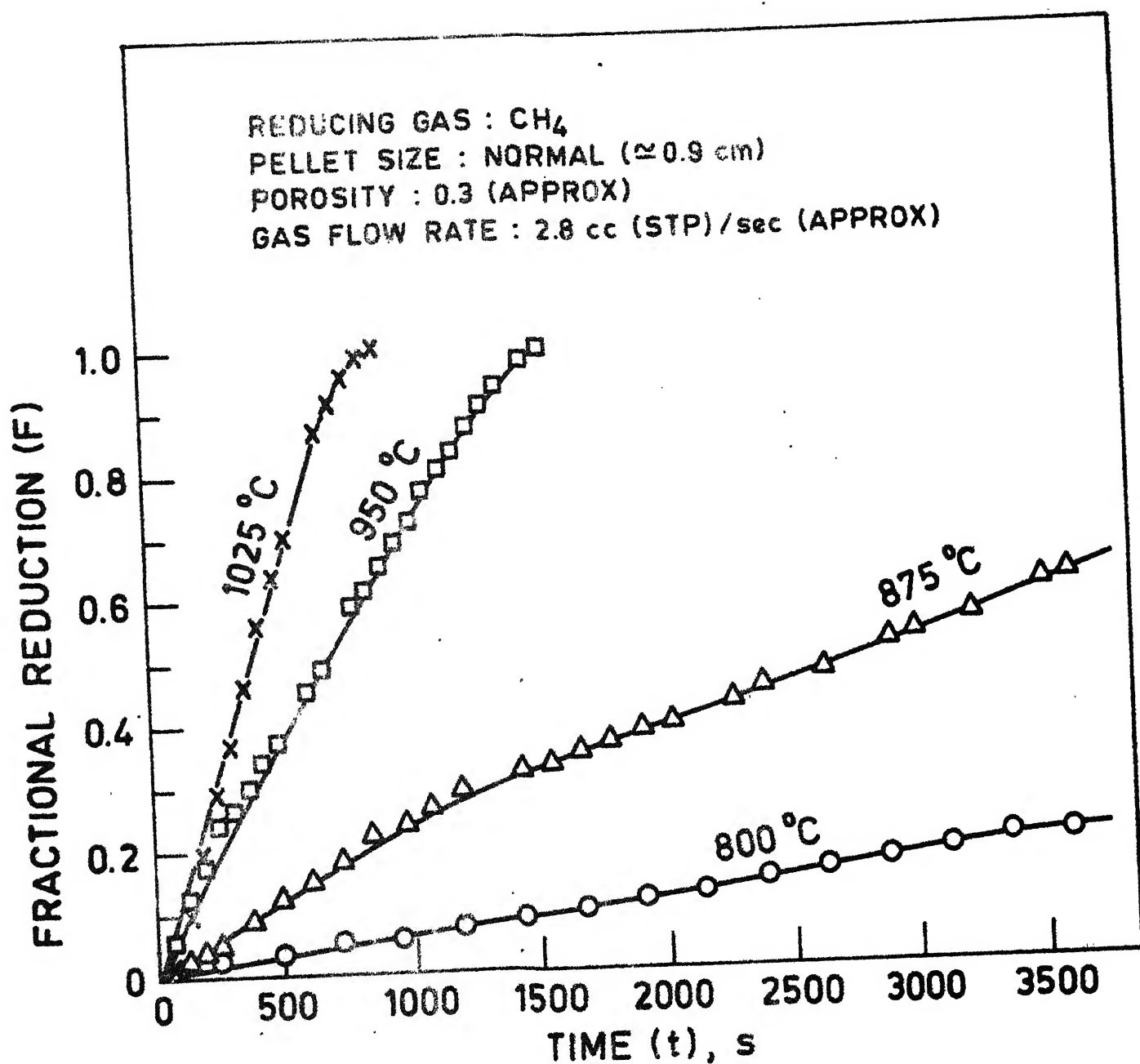


FIG. III.2 - EFFECT OF TIME AND TEMPERATURE ON FRACTIONAL REDUCTION WITH METHANE AT HIGH FLOW RATE.

U.S. GOVERNMENT
 GENERAL LIBRARY
 Acc. No. 65988

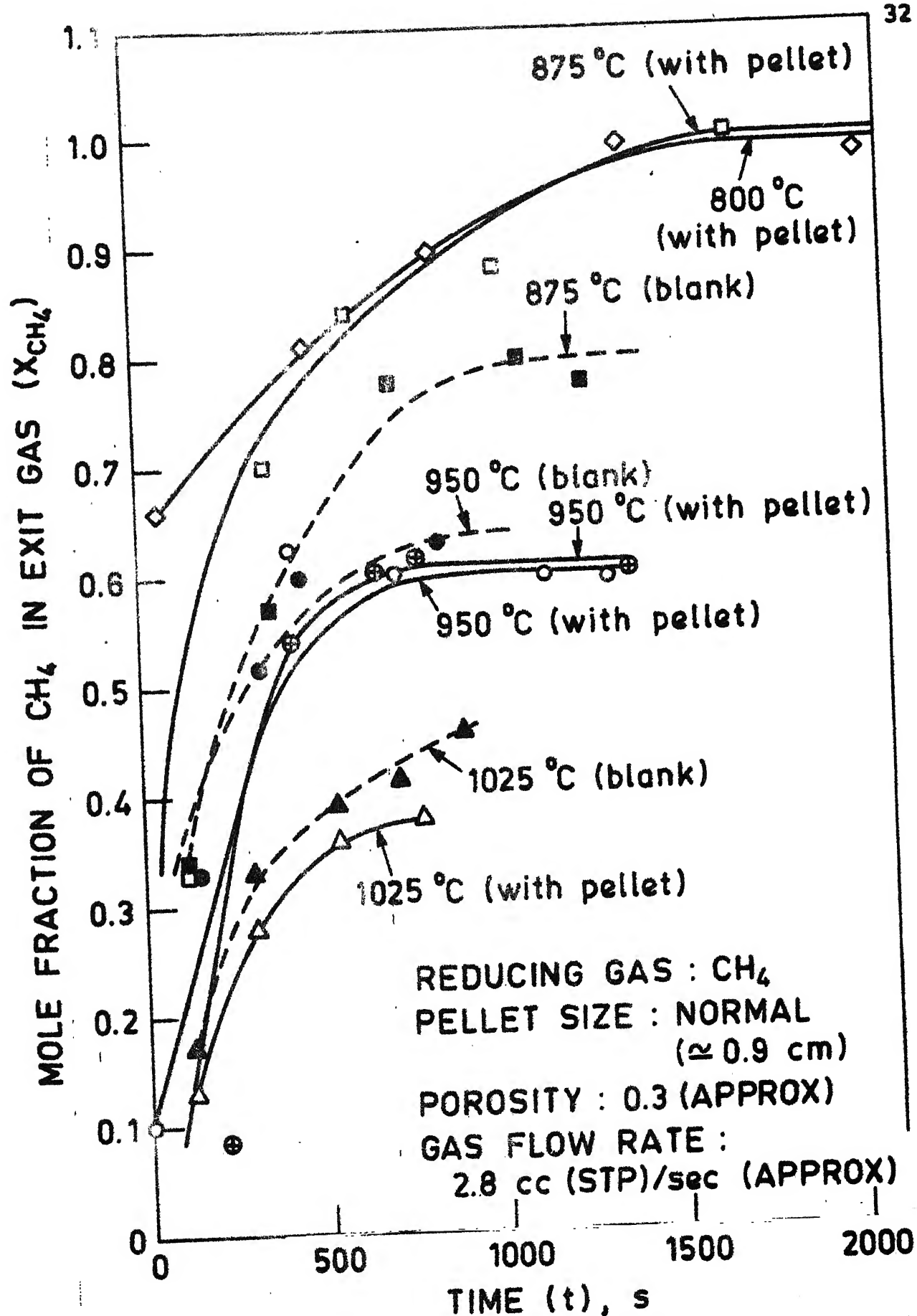


FIG. III.3 - VARIATION OF MOLE FRACTION OF CH_4 IN EXIT GAS WITH TIME AT DIFFERENT TEMPERATURES

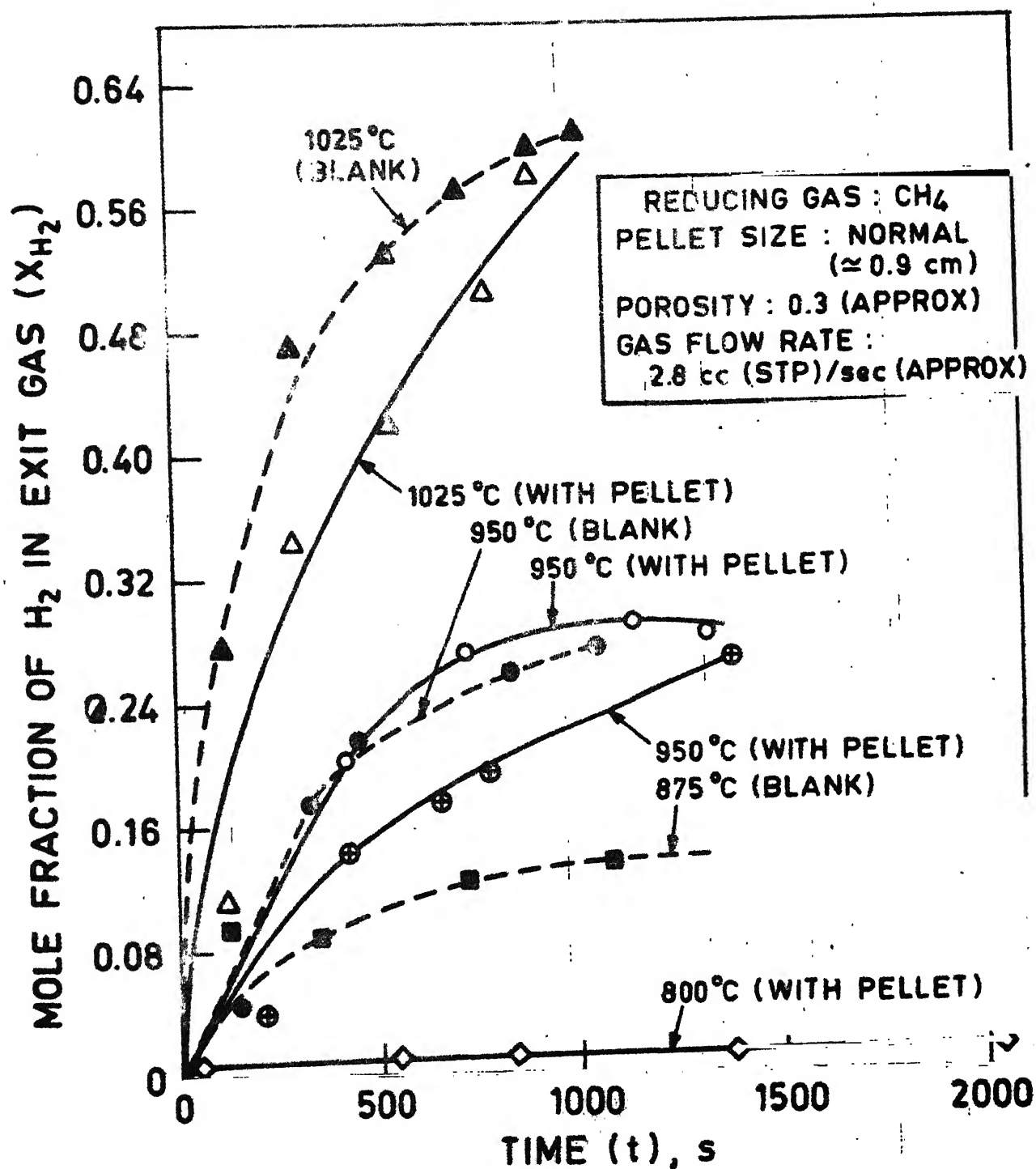
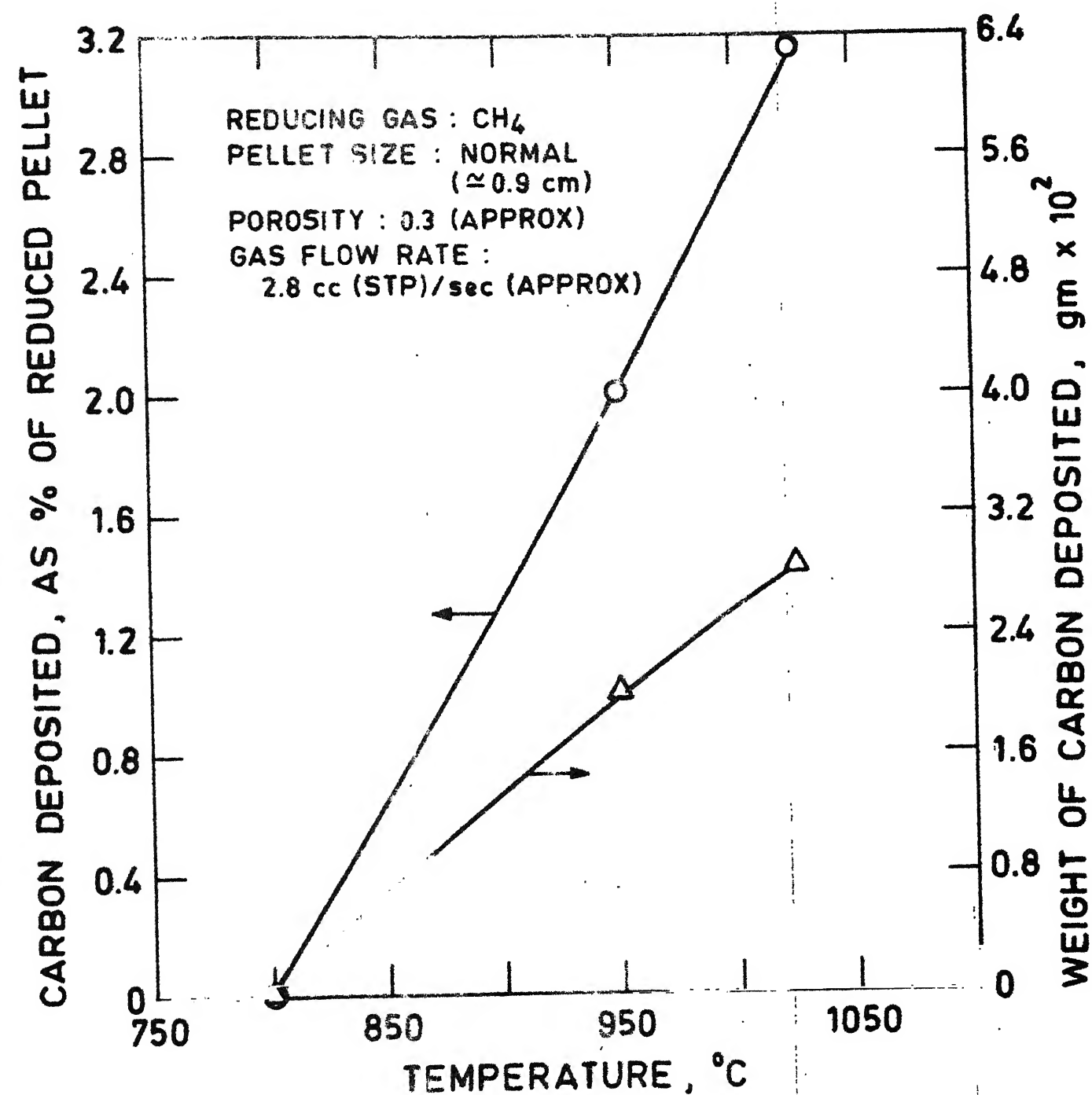


FIG. III.4 - VARIATION OF MOLE FRACTION OF H_2 IN EXIT GAS WITH TIME AT DIFFERENT TEMPERATURES.



G. III.5 - CARBON DEPOSITION ON PELLETS AT DIFFERENT TEMPERATURES.

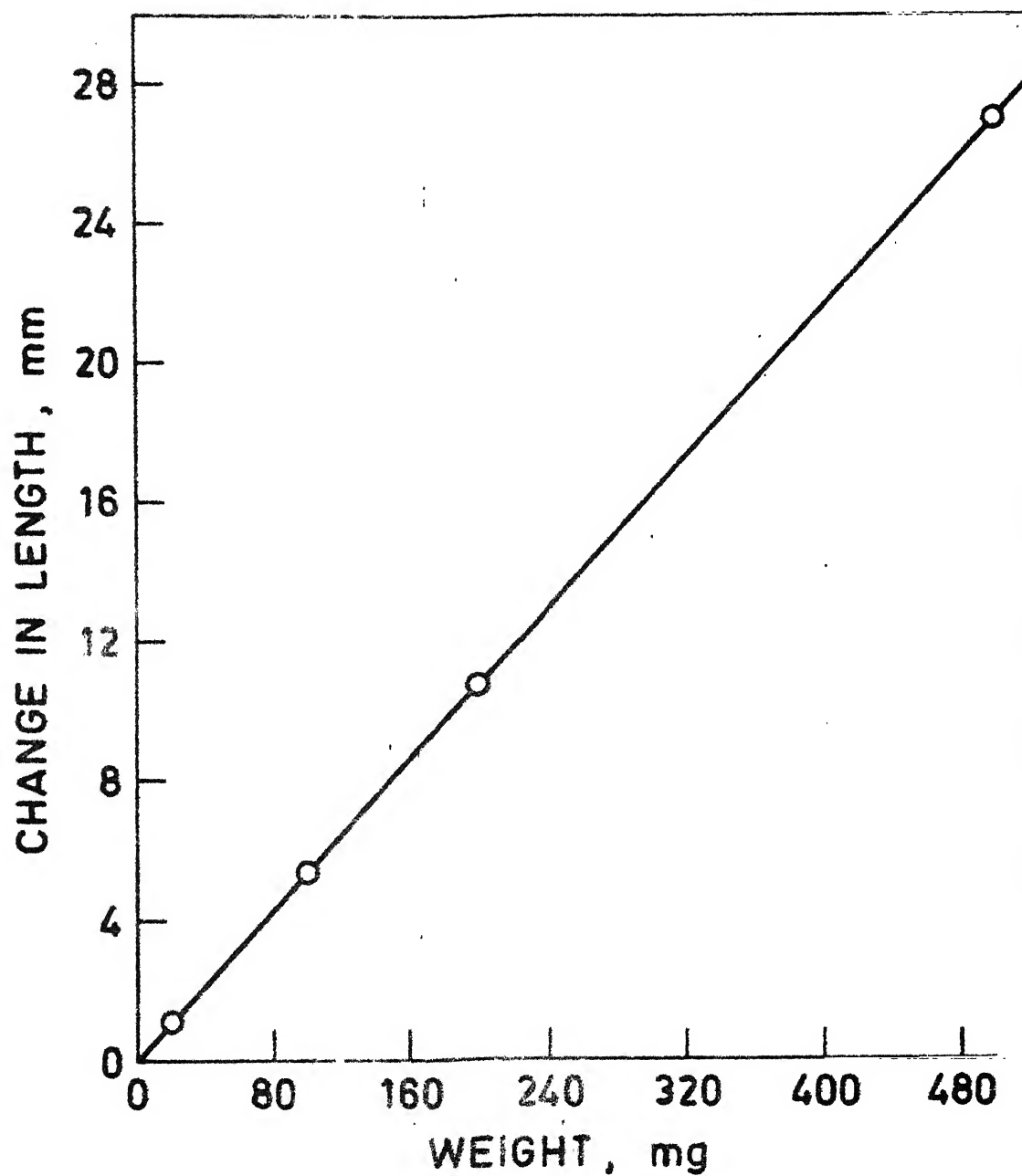


FIG. III.6 - TYPICAL SPRING CALIBRATION CURVE.

(e) Chromatographic gas analysis

: As mentioned in chapter II, the chromatograph was frequently calibrated using pure gases. Hydrogen, nitrogen, and argon were conveniently used as carrier gases in the gas chromatograph while analysing the exit gases during the reduction experiments. For first few experiments nitrogen was used as carrier gas. But the peaks of argon which was used as flushing gas in the reduction furnace were appearing at the position where carbon monoxide was supposed to come. To avoid these argon peaks, argon was simultaneously used as carrier gas in the chromatograph. But the problem with argon as carrier gas was its feeble response to detect CO_2 gas. Hydrogen was used as carrier gas when carbon dioxide detection was emphasized. Three chromatographic traces obtained by using the above three carrier gases are reproduced in fig. III.7. The volume of the gas sample injected, attenuation and identification of the peaks have been indicated in each chromatogram.

The error in gas analysis arises from the error in sample volume, inherent error of the chromatograph and recorder. Moreover, some errors creep into the measurement of peak areas. The overall error may be approximately taken as 6% - 8% of the values.

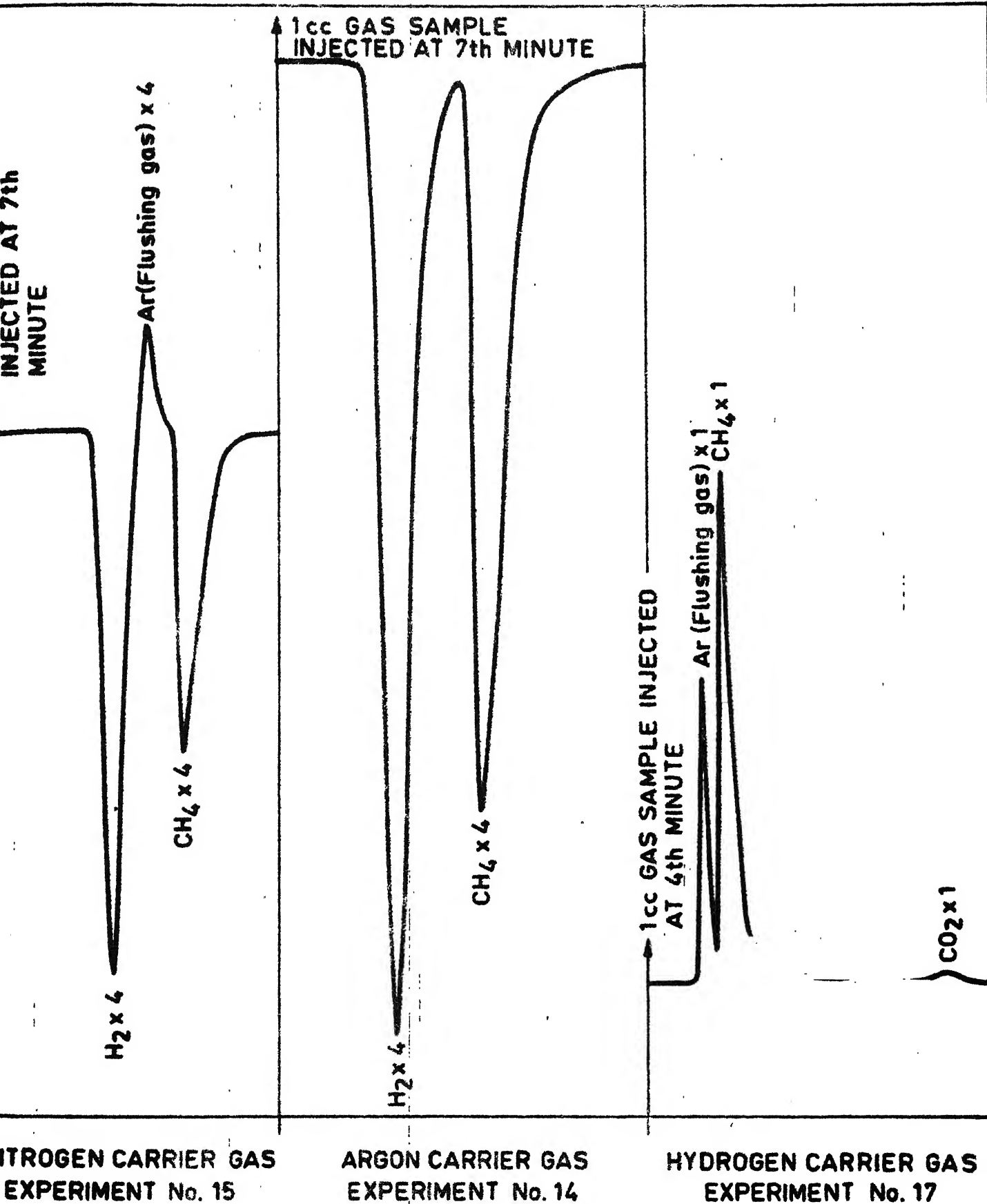


FIG. III.7 - CHROMATOGRAPHIC TRACES

(f) Carbon determination
on pellet

: The determination of carbon by passing oxygen in the furnace and absorption of resulting carbon dioxide by 'Indicarb' was found to be unreliable for a variety of reasons including suspected moisture pick up by 'Indicarb' during the process, small weight changes as compared to the weight of the Indicarb column, inability to oxidise carbon which penetrates inside the pellet etc. There were problems in determining carbon deposited on apparatus because some carbon deposition took place in the cooler temperature zone due to carry over by the gas. This carbon could not at all be converted into carbon dioxide. Therefore these data have been rejected and are not reported here.

The data reported here were collected by using the standard apparatus for determination of carbon in steel and cast iron. This apparatus had earlier been extensively calibrated for steel and cast iron samples by Rama Devi⁽¹⁵⁾. The accuracy may be taken as within $\pm 5\%$ of the value.

(g) Measurement of diameter of pellet

: Since the pellets were not exactly spherical, diameters were measured in various directions and averages were taken. The volume of a pellet was calculated from the average diameter data. The error in estimation of volume and porosity may be taken within $\pm 3\%$.

III.3 Reproducibility and Reliability of Measurements

Reproducibility of measurements was tested for hydrogen reduction of porous pellet at 800°C as shown in fig. III.8 and methane reduction of porous pellet at 950°C and 1025°C as shown in figs. III.9 and III.10.

As can be seen from the figures, reproducibility of thermogravimetric measurements for both hydrogen and methane have been fairly good. The slight discrepancies could be due to small differences in sizes and porosities from ^{pellet to} pellet. However, this could not be stated with certainty.

Basu and Ghosh⁽¹⁶⁾ determined fractional reduction vs. time for porous and dense pellets of ferric oxide in hydrogen at 800°C. Fig. III.8 compares the data of the present investigation with those reported by Basu⁽¹⁷⁾ for pellets of comparable porosities. It may be noted that the agreement is good. Since the data of Basu and Ghosh had agreed well with those of Mckewen⁽¹⁸⁾ for dense pellets, it may be concluded that the thermogravimetric set-up for the present investigation is quite reliable.

Reproducibility data of chromatographic gas analysis is presented in figs. III.3 and III.4.

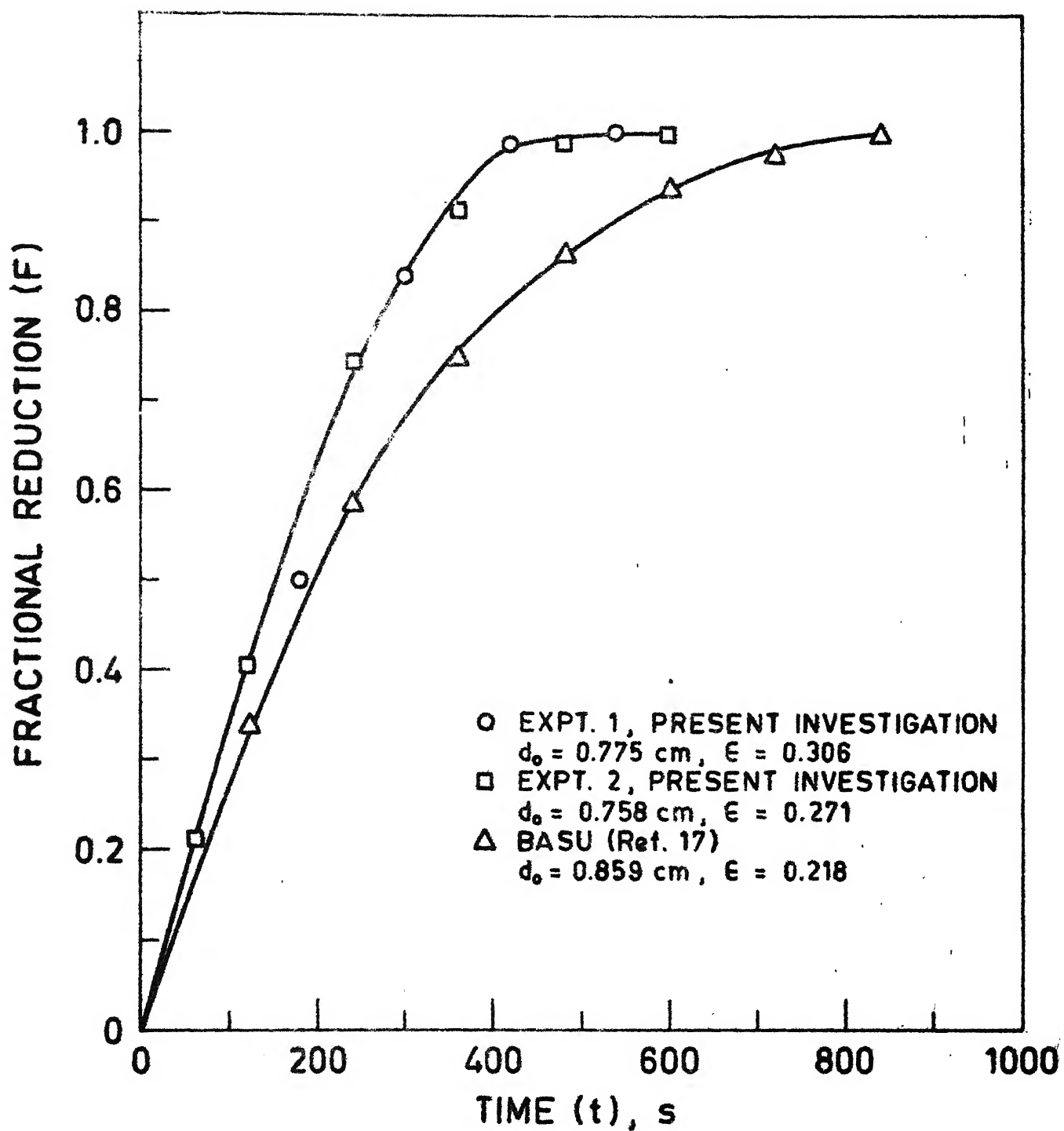


FIG. III.8 - FRACTIONAL REDUCTION vs TIME PLOTS FOR REDUCTION WITH H_2 AT $800^\circ C$.

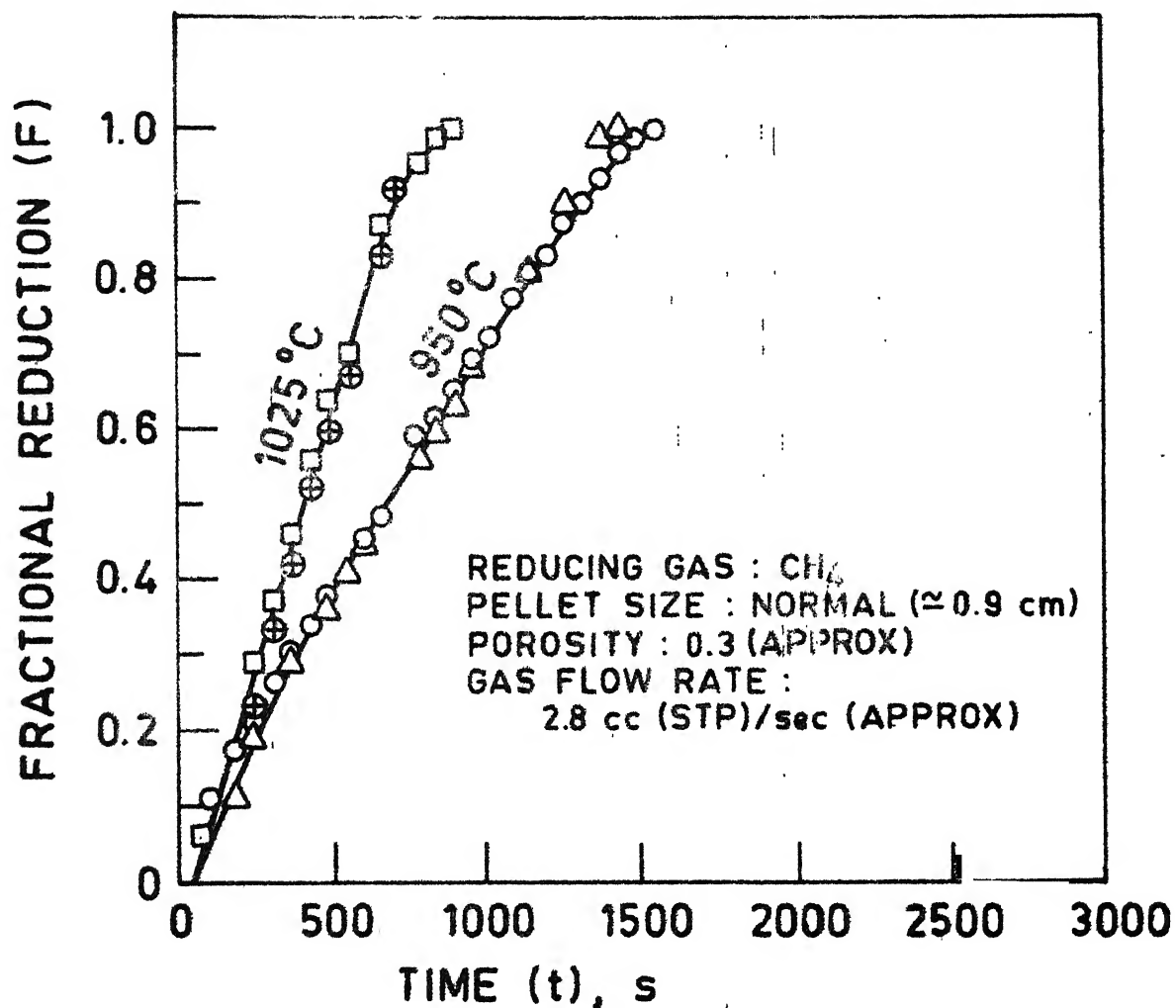


FIG. III.9 - REPRODUCIBILITY OF F vs t CURVES FOR REDUCTION WITH CH_4 AT HIGH FLOW RATE.

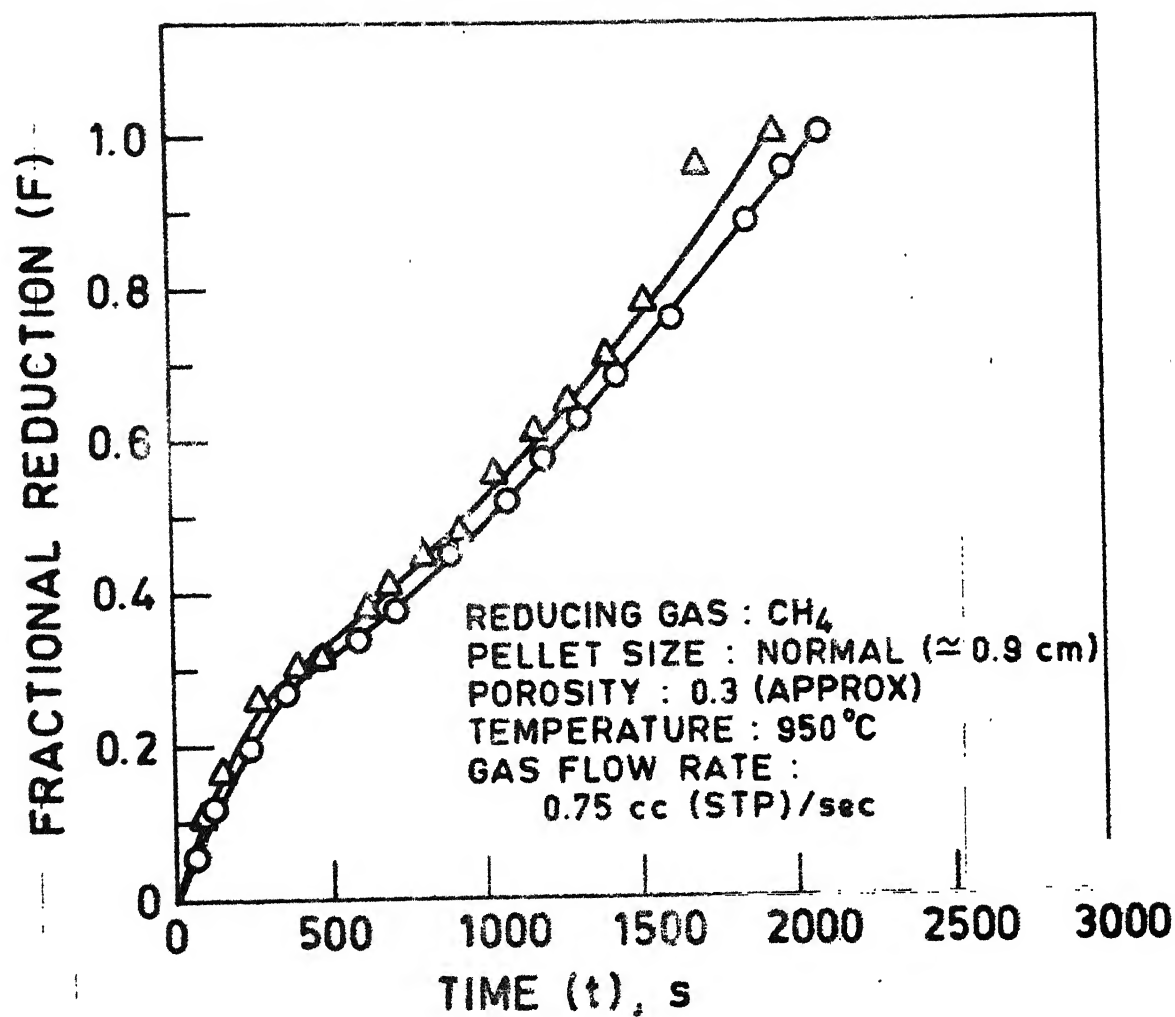
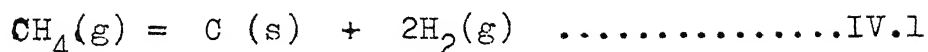


FIG. III.10 - REPRODUCIBILITY OF F vs t CURVES FOR REDUCTION WITH CH_4 AT LOW FLOW RATE.

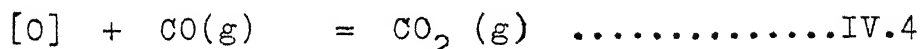
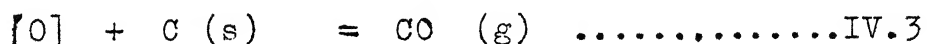
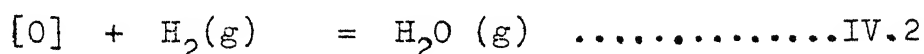
CHAPTER IV DISCUSSION OF RESULTS

A number of chemical reactions are expected to take place inside the furnace. These can be conveniently divided into the following three categories :-

(i) Decomposition of methane into carbon and hydrogen :

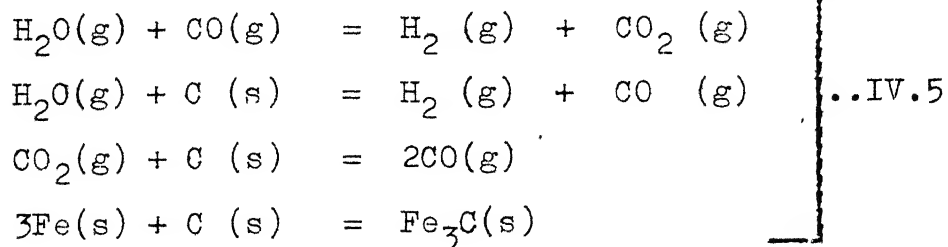


(ii) Reduction of iron oxide by hydrogen, carbon and carbon monoxide :



Here [O] denotes oxygen of iron oxide.

(iii) Auxiliary reactions :



IV.1 Decomposition of Methane

It can take place either on the pellet or in other parts of the apparatus (principally Mullite furnace tube).

Figs. III.3 and III.4 compare the variation of gas composition (i.e. methane and hydrogen) of exit gas as

a function of time for various temperatures (875°C , 950°C and 1025°C) with methane flow rate at about 2.8cc. (STP)/sec. Pellets of normal sizes (0.9cm. approx.) were used for reduction. These results have further been compared with the results of a few blank experiments where methane was passed under conditions identical to that of the original experiments but without using any pellet.

Figs. III.3 and III.4 reveal that both the concentrations of methane and hydrogen were very low at the beginning and tended to become steady as the reaction proceeded. This is presumably due to the delay in flushing out the inert gas from the furnace chamber. Initially the furnace chamber was full of inert gas. As flow of CH_4 was started, the concentration of CH_4 as well as that of H_2 resulting from the cracking of CH_4 started to increase. From the figures, it may be noted that it took 500 to 1000 seconds for the gas to attain steady state composition at 2.8cc. (STP)/sec. nominal flow rate of methane. The time to attain steady state gas composition was lower at higher temperature presumably due to the lower gas density at higher temperature.

Figs. III.3 and III.4 further show that at 950°C the concentrations of methane in blank as well as in experiments with ferric oxide pellets are fairly close. The hydrogen concentrations, however, show some variation. At 1025°C , both methane and hydrogen concentrations in the blank are higher than those in experiments with pellets. At 875°C , the methane concentration in the blank experiment was found to be lower than

those when ferric oxide pellet was present. Reliable data for comparison purposes were not available under other conditions. Anyway, it is clear from these results that there were substantial decomposition of methane even in the absence of the ferric oxide pellet. The lower concentration of hydrogen and methane with pellet at 1025°C can be reasonably explained by the presence of another gas (possibly carbon monoxide) which was detected by gas chromatograph. The somewhat lower hydrogen concentration in experiments with pellet at 950°C can not be explained off hand. However, it should be noted here that hydrogen analysis, in general, is expected to show more scatter than those encountered for other gases. Qualitatively speaking, these variations can be by and large attributed to minor variations in experimental conditions and perhaps some analytical errors.

All the above observations can be summed up by saying that the presence or absence of pellet did not alter the extent of decomposition of methane significantly. In other words, methane was decomposing mostly on the Mullite tube. This conclusion is corroborated by the fact that the amount of carbon deposited on the pellet was hardly few percent of the total carbon formed. For example, for experiment no.21, total carbon deposited is estimated as approximately 0.5gm, whereas the amount of carbon deposited on pellet was only 0.028gm(i.e. 7% of the total amount). Further evidences have been obtained by comparing the steady state gas composition during reduction of normal and big size pellet as well as of porous and dense pellet.

Results show that the steady state gas composition in each of the above cases is approximately same.

Theoretically the above observation can be justified by the fact that the surface area of the Mullite tube was larger than that of the pellet by 2 orders of magnitude. Metallic iron is likely to have some catalytic effect on decomposition of methane^(11,12). However, the surface area effect seems to be the predominating one.

Free energy of formation of methane from carbon and hydrogen are 43.796 KJ/mole at 950°C and 52.156 KJ/mole at 1025°C⁽¹³⁾. Equilibrium calculations at $p_{H_2} + p_{CH_4} = 1$ atm. reveals very small $(p_{CH_4})_{\text{equilibrium}}$ values which are 0.014 atm. and 0.006 atm. at 950°C and 1025°C respectively. Therefore, it can be concluded by comparing $(p_{CH_4})_{\text{equilibrium}}$ with $(p_{CH_4})_{\text{actual}}$ obtained from fig.IV.3 that the decomposition of methane in the furnace tube did not reach thermodynamic equilibrium at 950°C and 1025°C.

IV.2 Reduction Of Iron Oxide - Overall Considerations

Fig.IV.1 compares fractional reduction (F) vs. time (t) curves for reduction by hydrogen with that by methane at 950°C (experiment no.4 and no.14 respectively) for porous pellets. The rates of reduction (expressed as \dot{n}_O) were 0.066×10^{-3} and 0.014×10^{-3} g. atom oxygen/sec. respectively at $F = 0.7$. Therefore, the rate with hydrogen was about 4.5 times more than that with methane. Conclusions would be similar at other values of F. Similar observations were made by Misra⁽⁵⁾.

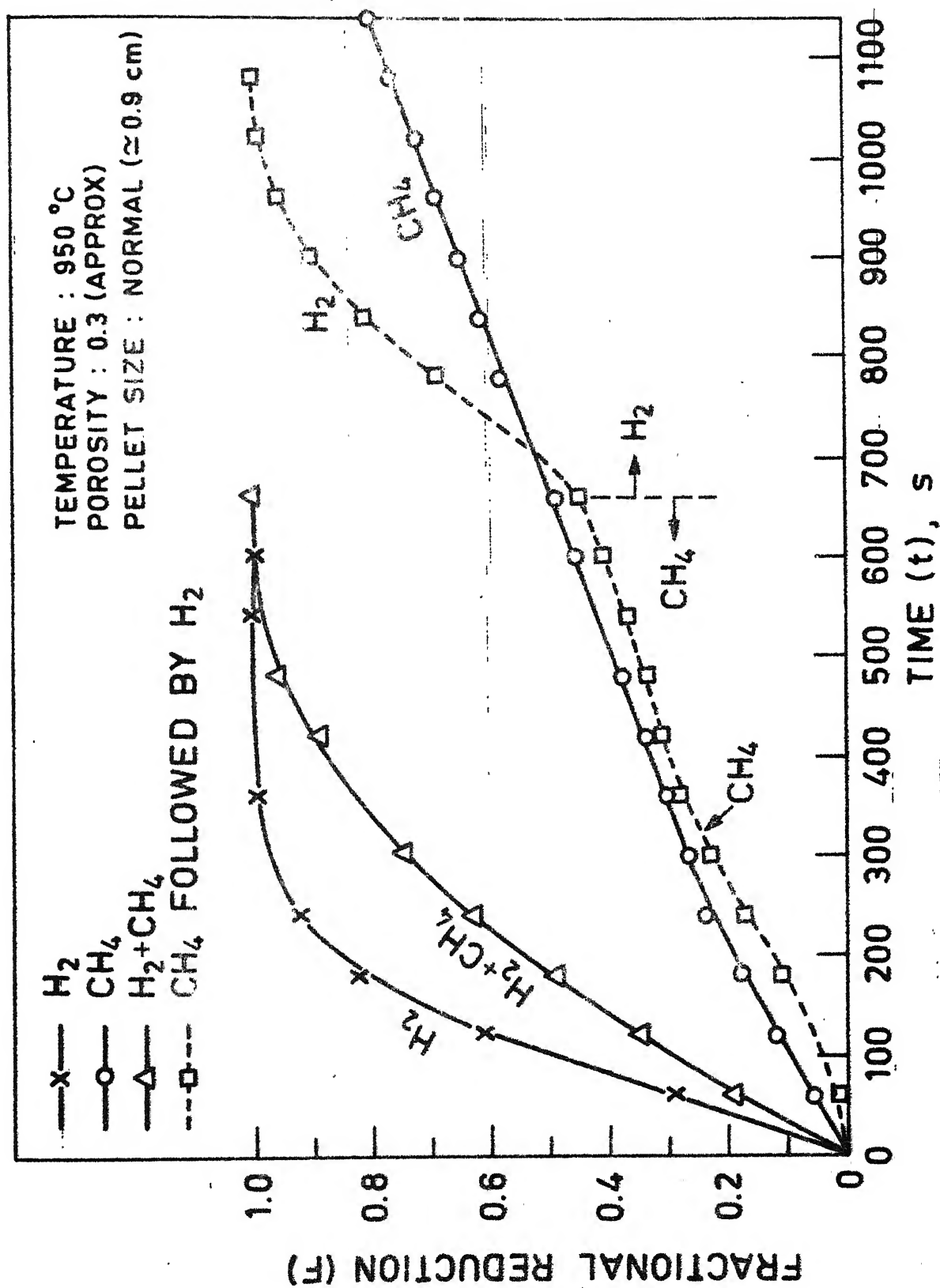


FIG. IV.1 - EFFECT OF TIME AND DIFFERENT REDUCING GASES ON FRACTIONAL REDUCTION .

Therefore the question that needs to be asked is- why is the reduction with methane so slow ? In order to answer this question we have to tentatively assume a mechanism of reduction. The mechanism being assumed is the decomposition of methane into carbon and hydrogen followed by the reduction of ferric oxide by hydrogen. Direct reduction of methane with oxide is ruled out as it would be too complex a reaction to take place in one step. Therefore, decomposition of methane is assumed to take place first. As hydrogen is six times faster reductant compared to carbon monoxide^(20,21) and even faster compared to carbon⁽²²⁾, therefore hydrogen is likely to be the primary reductant. The resultant H_2O may undergo one or more auxiliary reaction as given by equation IV.5. With the help of the above mechanism let us try to explain why reduction by methane is so much slower.

There ~~are~~ two possibilities to explain the above :-

(i) Blockage of pores by carbon deposited on the pellet :

It has been seen that the maximum carbon deposition is about 3 percent of the weight of the reduced metal, mostly much less. In porous pellets, base porosity has been approximately 0.3.

$$\begin{aligned} \text{Porosity after reduction} &= 1 - (1-\epsilon) \cdot \frac{2M_{Fe}}{M_{Fe_2O_3}} \cdot \frac{5.26}{7.8} \dots\dots IV.6 \\ &= 0.67 \end{aligned}$$

As a first approximation we can ignore the porosity developed during reduction, since its nature is complicated due to the presence of micro-or macro-porosity or due to the

phenomenon like swelling or shrinkage. In that case, weight of the reduced iron per unit volume of the reduced pellet = $5.26 \times \frac{112}{160} \times \epsilon = 1.10\text{gm.}$

Considering maximum carbon deposition of 3% of the weight of the reduced pellet,

the weight of the carbon deposited = $1.10 \times 0.03 = 0.033\text{gm.}$

Assuming density of carbon formed to be 1gm/cc , the maximum volume of carbon deposited becomes equal to 0.033 cc. This means that at the most 3% pore blockage takes place. This is too insignificant to explain so much lowering of reduction rate with CH_4 as compared to that with H_2 . However, it may be affecting in a minor way. To illustrate this, let us consider the experiment no.18 where methane was passed for some time and then it was switched over to hydrogen. As obtained from fig.IV.1, the reduction rate (\dot{n}_0) with hydrogen in this case at $F = 0.7$ was $0.052 \times 10^{-3}\text{ g. atom/sec.}$ It is little lower than that obtained by using hydrogen all through but still 3.5 times higher than the rate of reduction by methane. This is a further confirmation that the pore blockage by deposited carbon does not explain so much difference in rate of reduction by hydrogen and methane.

(ii) Reagent starvation effect in methane :

Fig.IV.2 compares F vs. t behaviour for porous pellet reduction at 950°C at two different flow rates of methane (0.75 cc(STP)/sec. and 2.77 cc(STP)/sec.). It may be noted that the reduction rate is higher at higher flow rate.

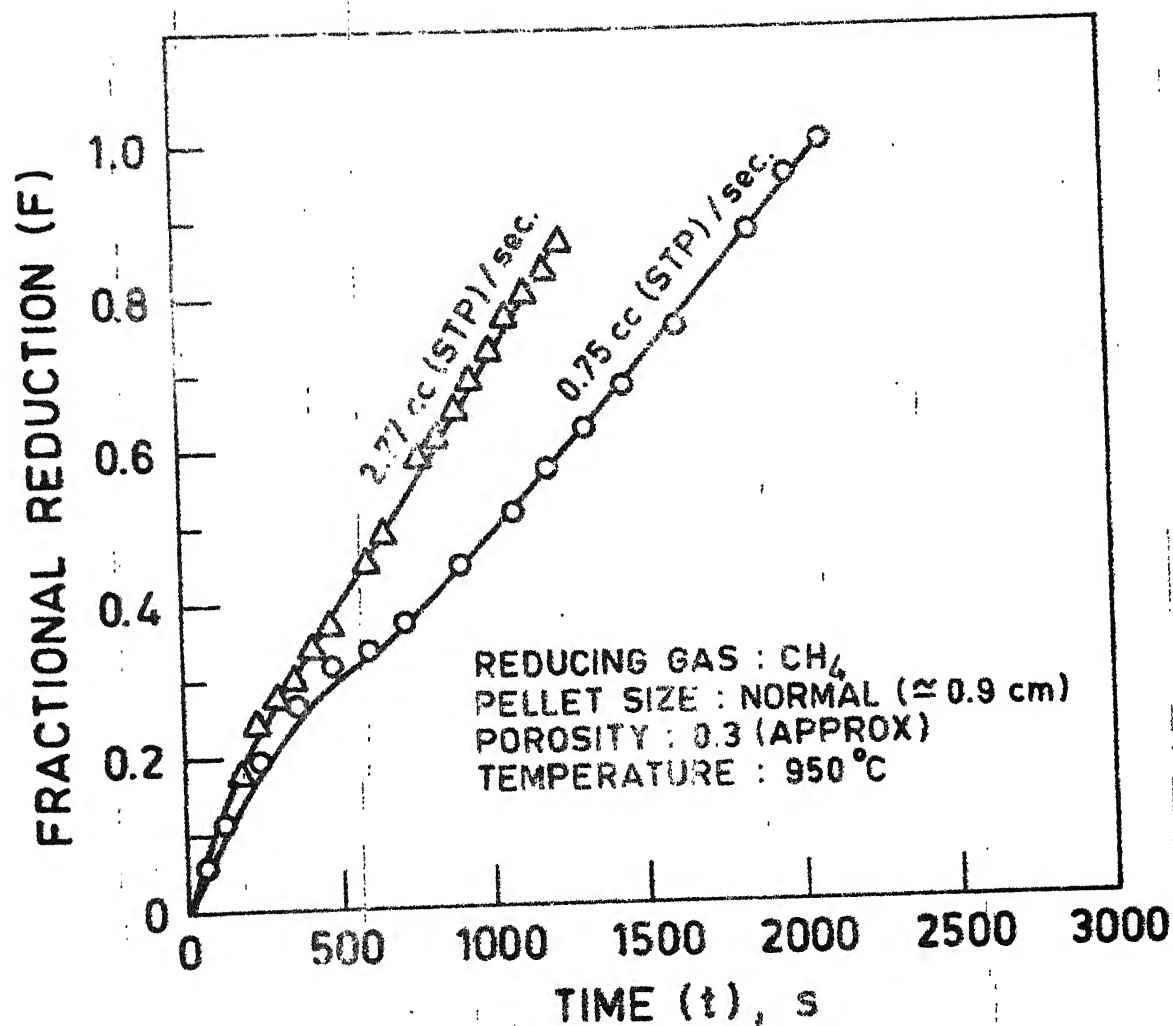
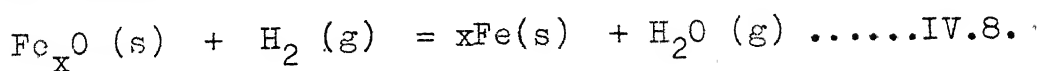


FIG. IV.2 - EFFECT OF TIME AND GAS FLOW RATE ON FRACTIONAL REDUCTION.

Hydrogen flow rate of 18.24 cc (STP)/sec. and methane flow rate of $\frac{18.24}{2}$ i.e. 9.12 cc(STP)/sec. would be stoichiometrically equivalent. In present investigation, the methane flow rate for most of the experiments was about 2.8 cc(STP)/sec. This is far lower as compared to the stoichiometric equivalent rate (9.12 cc(STP)/sec.). But how much increase in reduction rate with increase in flow rate of methane will occur is an important question.

Experiments and calculations by investigators^(23,24) on hydrogen reduction of iron ore showed conclusively that the rate becomes almost independent of flow rate above the 'minimum critical flow rate'. Minimum critical flow rate is decided by the 'reagent starvation effect' which happens when an appreciable build up of product gas (i.e. H_2O) takes place inside the furnace.

Moreover, as figs.III.3, and III.4 show, the concentration of methane and hydrogen were low to start with and built up to a steady value in approximately 500 - 1000 seconds with 2.8 cc(STP)/sec. methane flow rate due to slow flushing of inert gas. Therefore, there is a likelihood of reagent starvation in the initial period. To study this reagent starvation phenomenon $(p_{H_2O}/p_{H_2})_{\text{actual}}$ in the exit gas were calculated at different times and then compared with $(p_{H_2O}/p_{H_2})_{\text{equilibrium}}$, where, $(p_{H_2O}/p_{H_2})_{\text{equilibrium}} = K_{Fe-H}$ IV.7.
 K_{Fe-H} is the equilibrium constant for the reaction :



Calculation procedure to obtain $(p_{H_2O}/p_{H_2})_{\text{actual}}$ is presented in Appendix A.II. Table IV.1 presents values of $(p_{H_2O}/p_{H_2})_{\text{actual}}$ for different times at various temperatures and flow rates, and comparison of these with $(p_{H_2O}/p_{H_2})_{\text{equilibrium}}$ obtained from literature (19,25).

Calculations of $(p_{H_2O}/p_{H_2})_{\text{actual}}$ are unreliable for the initial periods as the results are very much sensitive to any minor error involved in the gas analysis. However, those are more reliable at later periods. By and large, values of $(p_{H_2O}/p_{H_2})_{\text{actual}}$ decreased with increasing time. Fig. IV.3 reveals that

$(p_{H_2O}/p_{H_2})_{\text{actual}} < (p_{H_2O}/p_{H_2})_{\text{equilibrium}}$ at 1025°C and 950°C, and

$(p_{H_2O}/p_{H_2})_{\text{actual}} \simeq (p_{H_2O}/p_{H_2})_{\text{equilibrium}}$ at 875°C and 800°C.

The above calculations show that there should not be much of a reduction to the metallic iron stage at 875°C and 800°C. However, it was possible to achieve a reduction of about 98 percent at 875°C in experiment nos. 12 and 16. This conclusively proves that the reduction at 875°C went to the metallic iron stage. Therefore, the $(p_{H_2O}/p_{H_2})_{\text{actual}}$ ratio must have been lower than the calculated values. Moreover, the H_2O concentration was supposed to be less due to the auxiliary reactions according to equation IV.5. Hence the above calculations are expected to yield H_2O concentration on the higher side, i.e. higher $(p_{H_2O}/p_{H_2})_{\text{actual}}$ than what it really

Comparison of (p_{H_2O}/p_{H_2}) Actual with (p_{H_2O}/p_{H_2}) equilibrium

Table IV.1

Temperature °C	(p_{H_2O}/p_{H_2}) Actual			(p_{H_2O}/p_{H_2}) Eqbm.	
	CH ₄ Flow Rate (0.75cc(STP))/sec.)			CH ₄ Flow Rate (2.8 cc(STP))/sec. approx.)	
	Initial Period	Intermediate Period	Towards End	Initial Period	Inter-wards to End
800	3.52	0.79	0.817	4.4	0.80 0.56
875	2.69	0.135	No gas analysis	2	0.61 0.81(φ)
950	α(φ)	0.45	No gas analysis	140(φ)	0.446 0.279
1025	Experiments	not done		8.46(φ)	0.39 0.15

(φ) Not reliable.

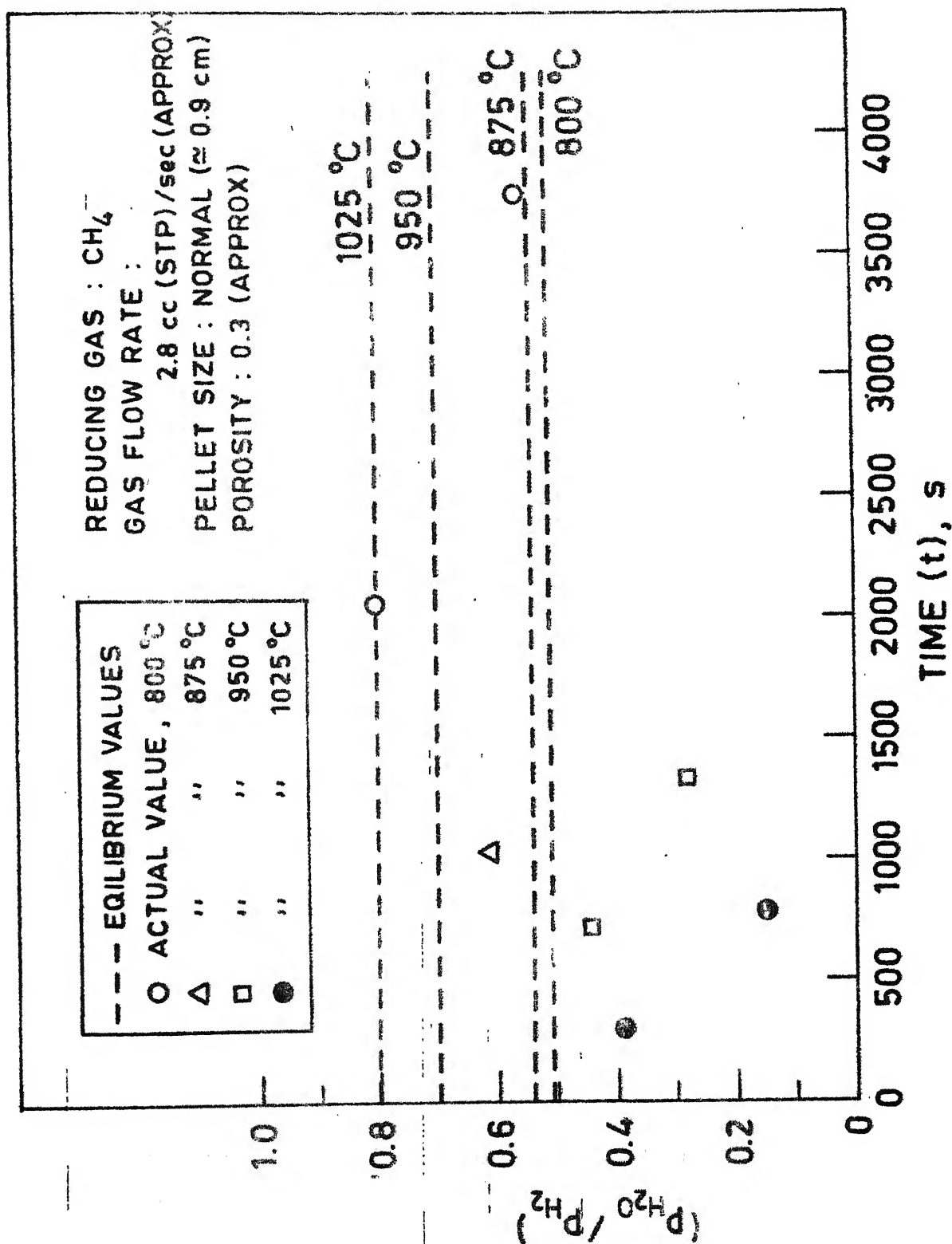


FIG. IV.3 - COMPARISON OF $(p_{\text{H}_2\text{O}}/p_{\text{H}_2})$ actual WITH $(p_{\text{H}_2\text{O}}/p_{\text{H}_2})$ equilibrium AT DIFFERENT TEMPERATURES.

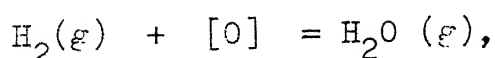
would have been. Therefore, beyond the initial period, especially at 950°C and 1025°C , significant reagent starvation is not expected. So one can safely conclude that with higher methane flow rate, no such drastic change of reduction rate would be observed. On the contrary, as discussed later in section IV.11, with too high flow rate of methane, reduction rate may be retarded.

IV.3 Analysis of Steady State Region

As already discussed in section IV.2, steady state region was the one where reduction rate as well as exit methane and hydrogen gas composition remained almost constant. From figs. III.1 and III.2 it can be seen that this region started after approximately 500 seconds to 1000 seconds and extended almost to the end of the reduction with 2.8 cc (STP)/sec. flow rate of methane. With 0.75 cc (STP)/sec. flow rate of methane this time was approximately 800 seconds to 2000 seconds. Moreover, there was no significant reagent starvation in this region especially at 950°C and 1025°C . So this region can be well employed for further analysis.

IV.3.1 Dependence of rate on p_{H_2} :

As has been stated earlier in section IV.2, hydrogen generated by cracking of methane has been assumed as the primary reductant. Recalling the hydrogen reduction reaction i.e. equation IV.2



it can be stated that the rate of reduction is proportional

to $(C_{H_2} - \frac{C_{H_2O}}{K})$. But, C_{H_2O} itself is proportional to rate of reduction. Hence, rate of reduction is proportional to C_{H_2} . This means rate is proportional to p_{H_2} when temperature is taken constant. Fig. IV.4 shows dependence of rate (i.e. \dot{n}_O) on p_{H_2} (in exit gas) when $F = 0.7$. This fig. IV.4 refers to experiment nos. 4, 14 and 19 which were conducted with porous pellets at 950°C . Here, p_{H_2} (in exit gas) has been taken as p_{H_2} (before the reaction). But, this is not a correct approach as it has been estimated that approximately 20/ to 30/ of the hydrogen, formed by methane cracking, was consumed by the reaction expressed by the equation IV.2. But nevertheless, as this is a common aspect of the experiments which are being considered, for comparison purpose, previous simplification can be done without committing much error. Moreover, it is not possible to obtain the p_{H_2} value before the reaction. With this approximation a linear dependence of rate with p_{H_2} has been obtained in fig. IV.4 which proves that the rate of reduction is proportional to p_{H_2} . This is in conformity with the mechanism postulated.

IV.3.2 Temperature dependence of reduction rate :

IV.3.2.1 Consideration of overall reaction:

Figs. IV.5 and IV.6 present $\log (\dot{n}_O \times 10^7)$ vs. $\frac{1}{T} \times 10^4$ plot to show temperature dependence of reduction rate. From the slope of this plot, ^{apparent} activation energy of the reduction reaction is obtained. Fig. IV.5 presents the plot for $F = 0.2$ with lower methane flow rate (i.e. 0.75 cc/sec.)

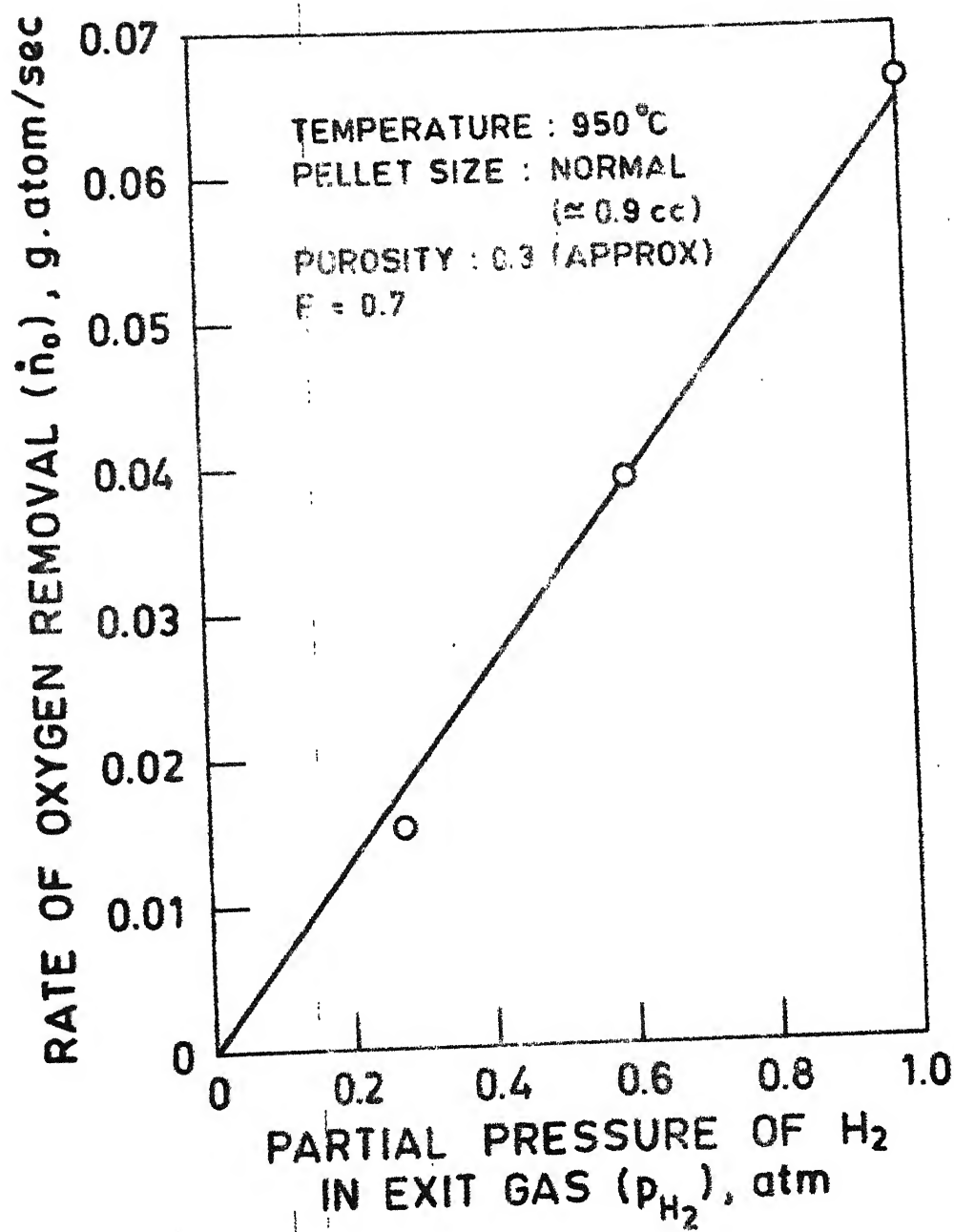


FIG. IV.4 - EFFECT OF PARTIAL PRESSURE OF H_2 IN EXIT GAS ON RATE OF OXYGEN REMOVAL.

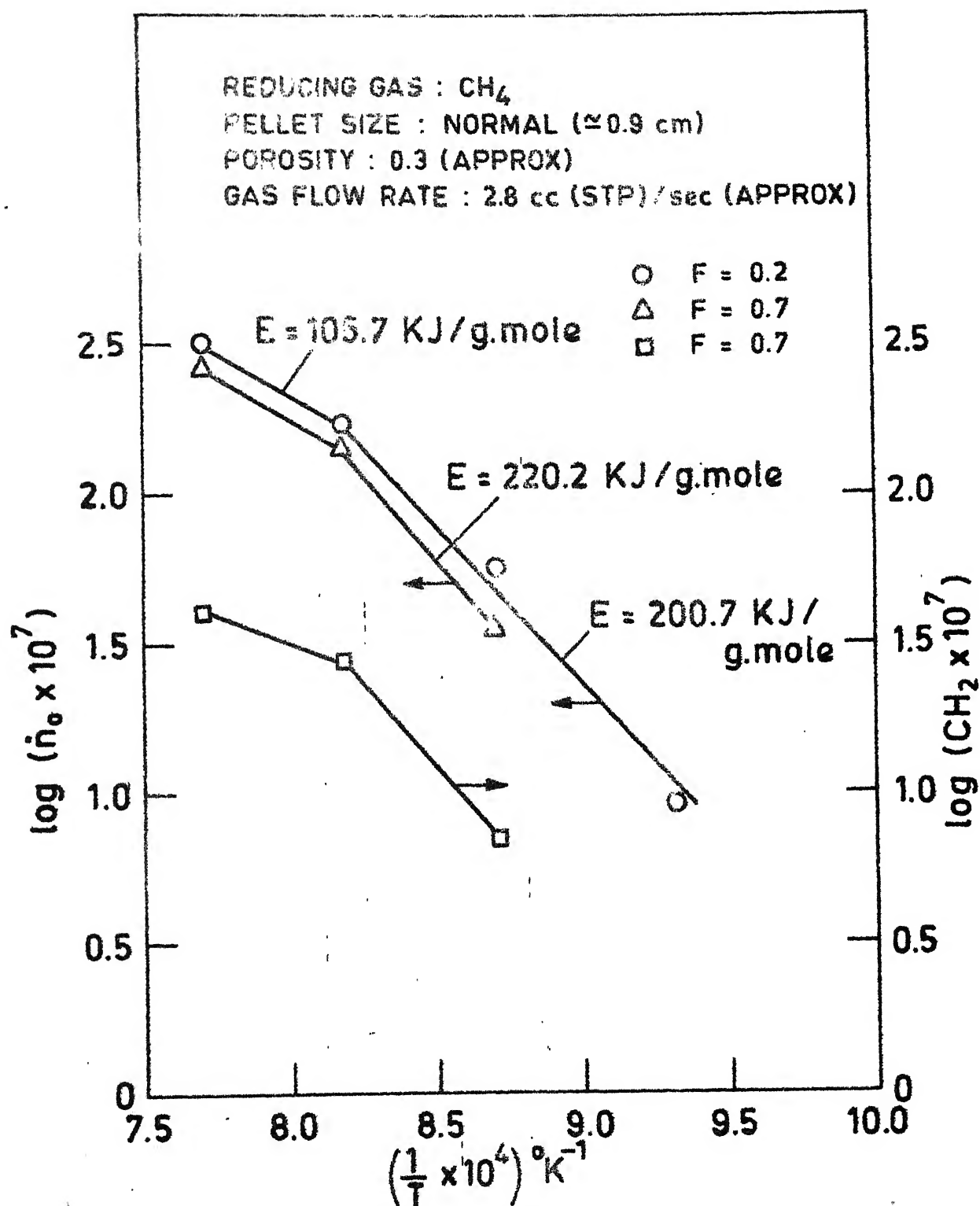


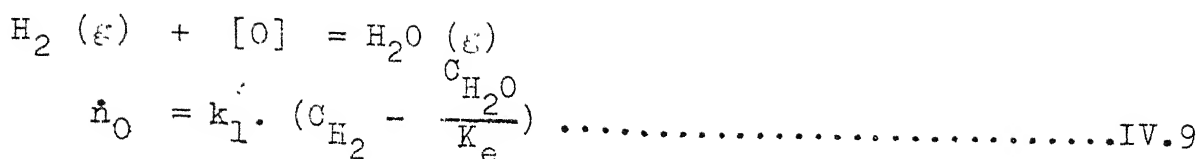
FIG. IV.6 - ARRHENIUS PLOT FOR REDUCTION AT HIGH FLOW RATE.

whereas fig.IV.6 presents the plots for $F = 0.2$ and $F = 0.7$ with higher flow rate of methane (i.e. 2.8 cc/sec.). From fig. IV.5, ^{apparent} activation energy value was obtained as 206.6 KJ/g.mole in the temperature range of $800^{\circ}\text{C} - 950^{\circ}\text{C}$ with lower flow rate of methane. With higher flow rate (fig.IV.6), ^{apparent} activation energy at both $F = 0.2$ and $F = 0.7$ was obtained as 105.7 KJ/g.mole in the temperature range of $950^{\circ}\text{C} - 1025^{\circ}\text{C}$. It was 200.7 KJ/g.mole in the temperature range of $800^{\circ}\text{C} - 950^{\circ}\text{C}$ at $F = 0.2$ and 220.2 KJ/g.mole in the temperature range $875^{\circ}\text{C} - 950^{\circ}\text{C}$ at $F = 0.7$. This sort of nature might be due to different rate controlling steps at different temperature ranges.

Fig.IV.6 also shows the variation of exit gas H_2 concentration with temperature as $\log C_{\text{H}_2}$ vs. $\frac{1}{T} \times 10^4$ plot at $F = 0.7$. Experimental conditions for $\log (\dot{n}_0 \times 10^7)$ and $\log (C_{\text{H}_2} \times 10^7)$ vs. $\frac{1}{T} \times 10^4$ plot were exactly same which would be helpful for comparison purpose. These two curves are almost parallel. Following this observation, variation of rate of reduction with temperature can be greatly attributed to variation of concentration of H_2 with temperature. It can also be concluded that the decomposition of CH_4 (eqn.IV.1) is controlling the overall rate largely.

IV.3.2.2 Consideration of reduction reaction :

Let us now consider the reaction which follows the decomposition of CH_4 according to the postulated mechanism. This is the reaction expressed by the equation IV.2 as,



$$= k_1 \cdot C_{\text{H}_2} \text{ [as, } C_{\text{H}_2\text{O}} \text{ is proportional to } \dot{n}_0]$$

$$= k_1 \cdot \frac{P_{\text{H}_2}}{RT}$$

$$\text{At } P_T = 1 \text{ atm., } P_{\text{H}_2} = X_{\text{H}_2}$$

$$\text{so, } \dot{n}_0 = k_1 \cdot \frac{X_{\text{H}_2}}{RT} \dots\dots\dots \text{IV.10}$$

Table IV.2 presents the values of \dot{n}_0 , $\frac{X_{\text{H}_2}}{RT}$ and k_1 at $P=0.7$ for porous pellet reduction at different temperatures.

Table IV.2

Calculations of k_1 at different temperatures

<u>T, °K</u>	<u>F</u>	<u>\dot{n}_0, g.atom/sec.</u>	<u>X_{H_2}</u>	<u>$C_{\text{H}_2} (= \frac{X_{\text{H}_2}}{RT})$, g.mole/cc</u>	<u>k_1, cc/sec.</u>
1298	0.7	0.259×10^{-4}	0.42	3.9×10^{-6}	6.63
1223	0.7	0.138×10^{-4}	0.28	2.7×10^{-6}	5.13
1148	0.7	0.033×10^{-4}	0.07	0.7×10^{-6}	4.67

Fig.IV.7 shows the plot of $\log k_1$ vs. $\frac{1}{T} \times 10^4$ from which apparent activation energy for the equation IV.9 was obtained as 45.0 KJ/g.mole in the temperature range of 950°C - 1025°C and 15.3 KJ/g.mole in the temperature range of 875°C - 950°C.

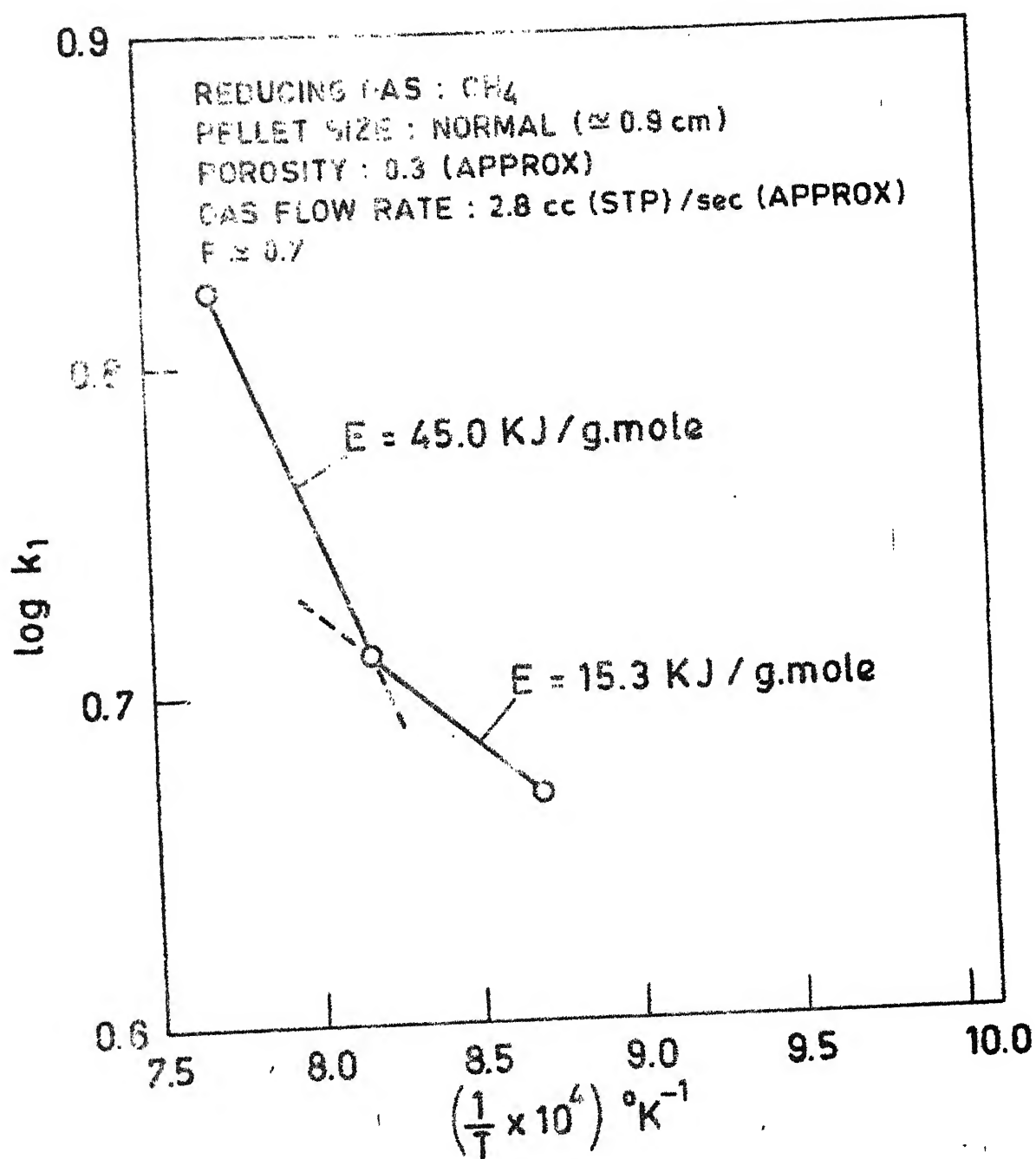


FIG. IV.7 - $\log k_1$ vs $1/T$ PLOT AT HIGH FLOW RATE.

IV.4 Nature of F vs. t Curves

In case of reduction of Fe_2O_3 by pure H_2 F vs. t curves dropped steadily, whereas, with CH_4 as reductant, these curves have shown a reproducible tendency of steady reduction rate sometimes after reduction starts, as has been told earlier (Fig.IV.1). This steady rate zone has appeared at all the reduction temperatures and with both high and low flow rate of methane. This constancy of the reduction rate for an appreciable period does not seem to be due to 'reagent starvation' effect as discussed earlier.

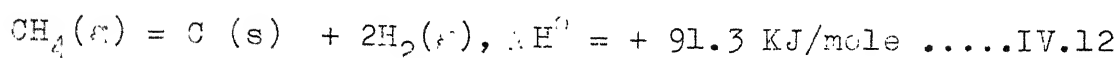
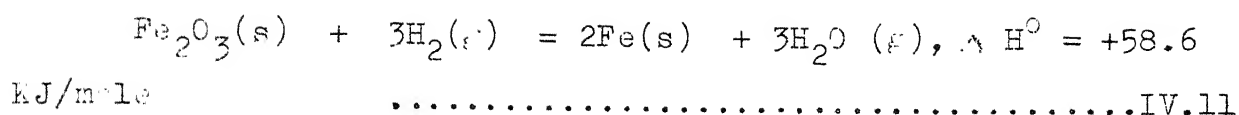
IV.5 Carbon Deposition on Pellets

Fig.III.5 shows the percentage as well as total amount of carbon deposition on pellet as a function of temperature. From the figure, it is obvious that the amount of carbon deposition drops with ^{drop in} temperature as was expected. In this connection, it should be noted that the carbon deposition data at 800°C corresponded to $F \sim 0.23$ whereas F was approximately 1.0 at both 950°C and 1025°C . However, the nature of the graph would have not changed much had the reduction at 800°C been extended upto $F \approx 1.0$. This is due to insignificant cracking of CH_4 at 800°C . Few experiments were carried out to measure the amount of carbon which had penetrated to the core of the pellet. Table III.1 shows that there were good penetration of the carbon to the core, especially at higher temperatures like 1025°C .

IV.6 Change of Temperature inside Pellet during Reduction

Some experiments (no.27 and no.28) were carried out to record the changes in temperature that occur inside the ferric oxide pellet during its reduction. The first experiment was carried out by embedding a chromel-plumel thermocouple in the centre of a pellet having a fractional porosity of 0.12. The change in temperature during the reduction of the pellet at 950°C by CH_4 with a flow rate of approximately 2.8 cc(STP)/sec. was measured at a regular interval. The decrease in the temperature went to the extent of 30°C in 1900 seconds with some intermediate fluctuation presumably due to severe pellet cracking. The second experiment was run as a blank one (i.e. without any pellet) to take care of the change of temperature due to decomposition of methane within the furnace. Though decomposition of methane is an endothermic reaction⁽¹⁹⁾, this experiment surprisingly recorded an increase in temperature of about 9°C in approximately equivalent time. This may be due to difference in heat capacity of methane from that of argon which was used as the flushing gas in both the experiments. This argument is justified by the temperature increase of approximately 6°C when argon was again switched on to replace methane.

So from the above discussion it is clear that a substantial temperature drop takes place inside the pellet during the reduction. This is due to the endothermic nature of the reactions. Heats of reactions are as follows⁽¹⁹⁾,



As methane decomposes mainly on the Mullite furnace tube surface, the endothermic reaction IV.11 is largely responsible for the temperature drop inside the pellet.

IV.7 Volume Changes in Pellet upon Reduction

Table IV.3 presents the overall picture regarding volume changes in pellet upon reduction. From this table it is clear that the reduction with H_2 caused a decrease in volume whereas reduction with CH_4 always increased the volume of the pellet, except at 1025°C . It is well-known that carbon deposition causes swelling of pellets during reduction. On the other hand sintering effect causes reduction in volume. In general, changes in volume of pellet upon reduction are caused by dynamic balance of various phenomena. Therefore no explanation could be attempted further.

IV.8 Comparison of Reduction of Dense and Porous Pellets

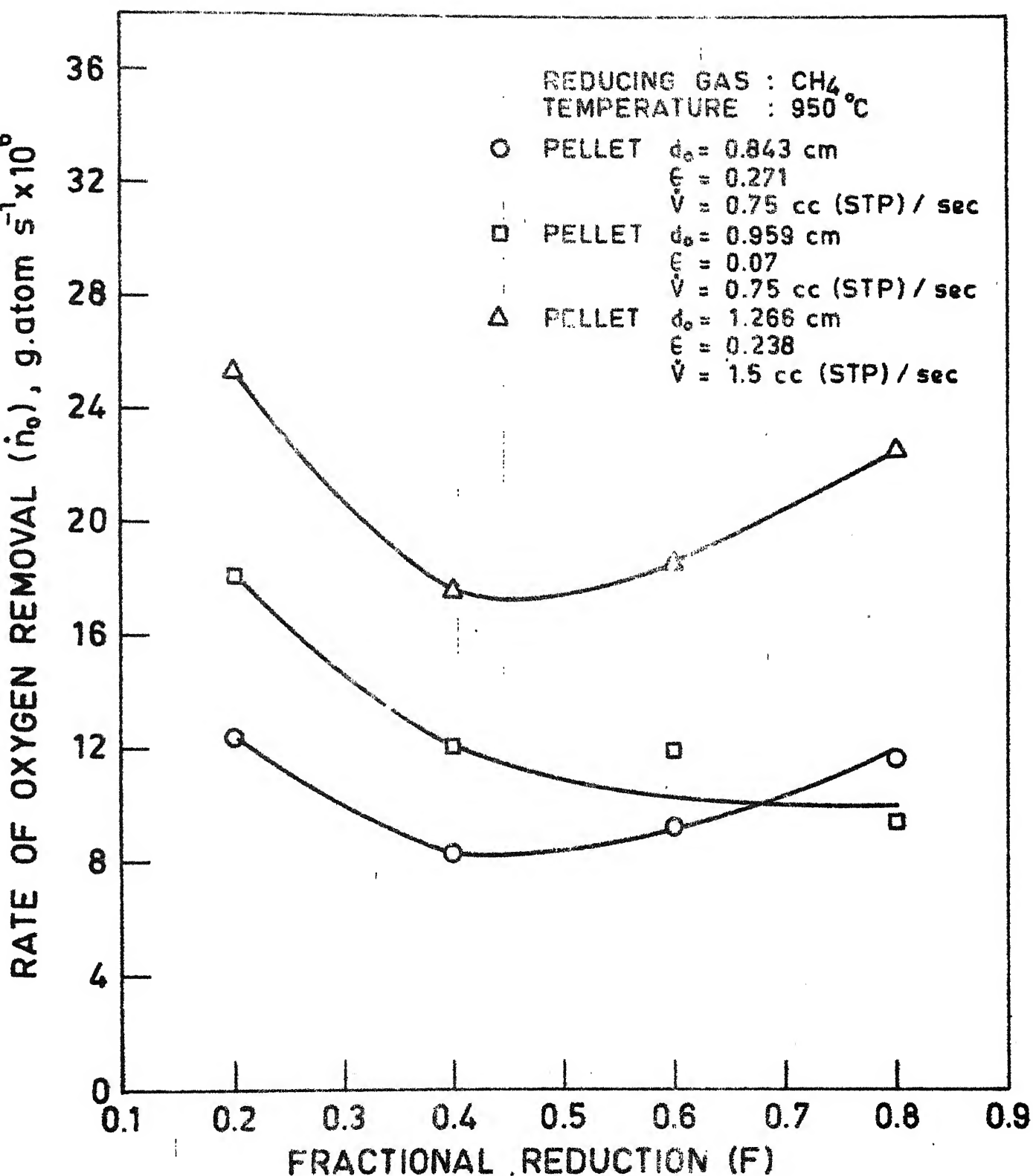
Figs. IV.8 and IV.9 present the plots of \dot{n}_0 vs. F to compare the reduction behaviour of dense and porous pellets at both low and high flow rate of CH_4 respectively. As may be noted from the above mentioned figures, the rates of oxygen removal with dense pellet were more than those with porous

Table IV.3 Size changes in pellet upon reduction

<u>Reducing Gas</u>	<u>Expt.No.</u>	<u>Temp., °C</u>	<u>ϵ</u>	<u>Original Dia. of The Pellet (d_o), cm.</u>	<u>Dia. of The Reduced Pellet (d_r), cm.</u>
H ₂	4	950	0.346	0.802	0.707
	3	800	0.067	0.963	0.898
CH ₄	21	1025	0.337	0.873	0.869
	25(φ)	1025	0.303	0.865	0.840
	8	950	0.070	0.959	1.126
	11	950	0.238	1.266	1.426
	15	950	0.299	0.848	0.937
	(η)	875	0.336	0.873	0.900
	20(φ)	800	0.253	0.838	0.855
CH ₄ +H ₂	19	950	0.304	0.876	0.816
CH ₄ followed by H ₂	10	950	0.251	0.837	0.841

(η) This experiment has not been included in the summary table III.1 as the run was interrupted after a fractional reduction (F) of 0.56.

(φ) These experiments were not carried upto $F \geq 1$, as had been done in other cases. For experiment no. 25 and 20, F was 0.72 and 0.23 respectively.



G. IV.8- \dot{n}_0 vs F PLOT FOR DIFFERENT SIZE AND POROSITY AT LOW GAS FLOW RATE.

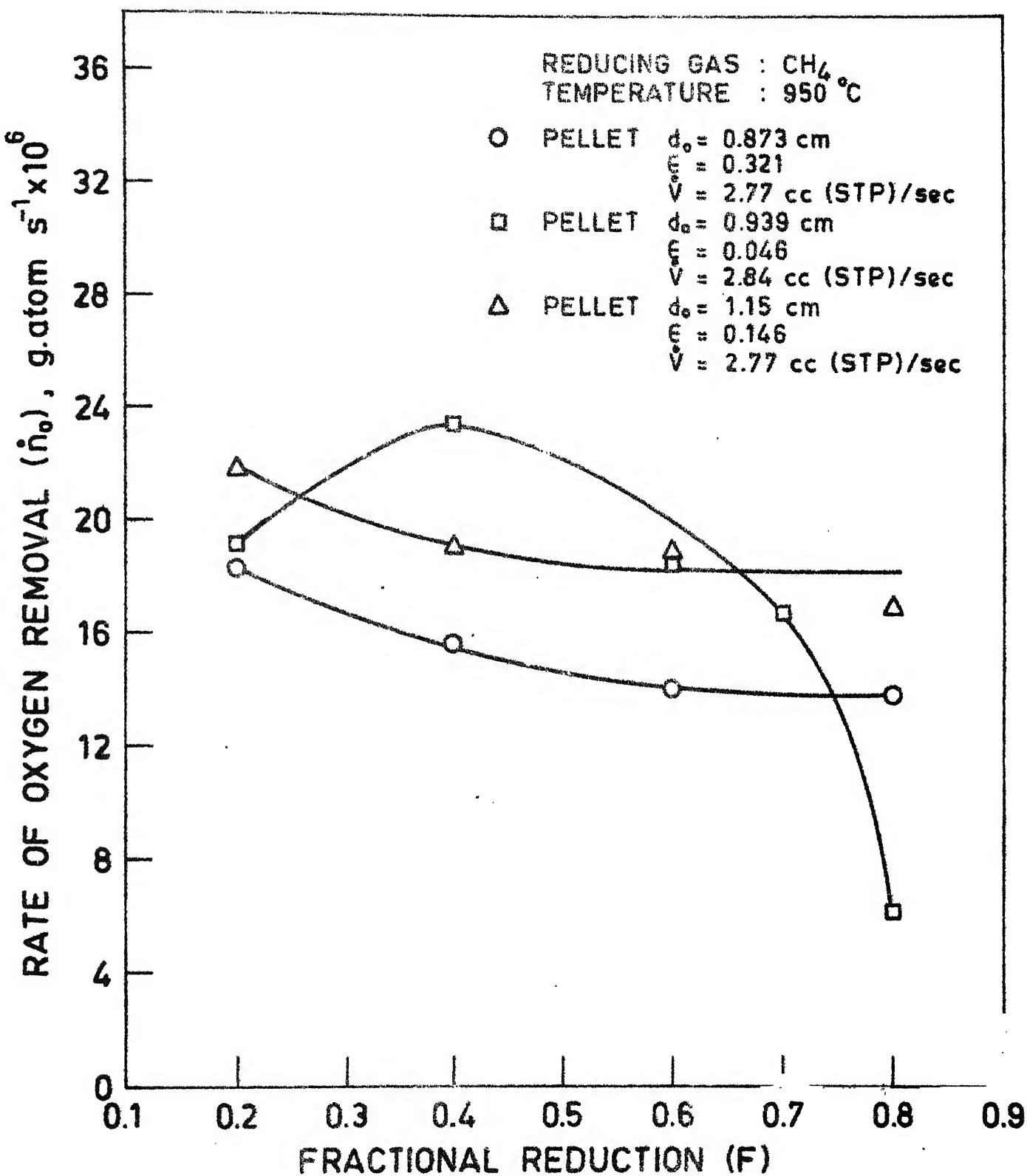


FIG. IV.9 - \dot{n}_0 vs F PLOT FOR DIFFERENT SIZE AND POROSITY AT HIGH GAS FLOW RATE.

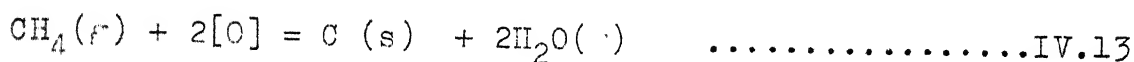
pellet for most of the times.

IV.9 Comparison of Reduction of Big and Normal Porous Pellets

Figs. IV.8 and IV.9 present the necessary plots of \dot{n}_O vs. F from which (the effect of size of pellet on reduction rate at both low and high flow rate of CH_4 is obtained. The reduction rate was more with the bigger pellet.

IV.10 Rate Controlling Step for Oxide Reduction

It has been discussed before that the overall reaction i.e.



was to a large extent controlled by the CH_4 decomposition reaction (equation IV.1). Let us now see what is the rate controlling step for the actual reduction reaction i.e.



Various possible kinetic steps for the reaction IV.2 are as follows :

- (i) Inward diffusion of H_2 through the gas boundary layer around the pellet.
- (ii) Inward diffusion of H_2 through the pores of the pellet.
- (iii) Chemical reaction (equation IV.2) at the iron/wustite interface.
- (iv) Outward diffusion of H_2O through the pores of the pellet.
- (v) Outward diffusion of H_2O through the gas boundary layer around the pellet.

Linearity of F vs. t plots from $F \approx 0.3$ to $F \approx 0.9$ in all the cases indicates that the rate is controlled by diffusion through the gas boundary layer. This constancy of rate can not be attributed to the reagent starvation effect which has been proved to be absent especially at 950°C and 1025°C , as shown in table IV.1. Also, this constancy can not be expected from a reaction controlled either by the pore diffusion or by the interfacial chemical reaction because in these two cases the nature of F vs. t curves would have been drooping.

Fig. IV.2 shows an increase in reduction rate with increase in flow rate. Apparently, this observation corroborates a rate control by diffusion through the gas film. But, in the experiments on reduction by H_2 (23,24), it has been found that the change in the flow rate alters the reagent starvation effect principally without affecting the mass transfer coefficient in the gas boundary layer. Above the 'critical flow rate' the rate becomes insensitive to flow rate because neither reagent starvation nor mass transfer coefficient is significantly affected by flow rate variation. Therefore, it would not be wise to make any conclusion about the rate controlling step, based upon the effect of flow rate on the rate of reduction.

Figs. IV.8 and IV.9 show that at 950°C , the rates of reduction with the dense pellets were, in most of the times, higher than those with the porous pellets of comparable size and at comparable flow rate of CH_4 . This is not to be expected

from a reaction controlled by diffusion through the pores, because with porous pellets, a higher reduction rate would have been obtained.

Figs. IV.8 and IV.9 also compare the reduction rates of pellets of two different sizes in otherwise similar conditions. In the steady state region at 950°C , it has been seen, with the results from experiment nos.14 and 26, that \dot{n}_0 is proportional to the diameter of the pellet (d_0). This is possible if the pore diffusion was rate controlling step. For the rate being controlled by diffusion in the gas boundary layer, \dot{n}_0 should be proportional to d_0^2 . This apparently contradicts what have been discussed previously. However, it is to be noted that the bigger pellet in experiment no. 26 did not have the desired fractional porosity ($\epsilon = 0.3$). It is likely that due to its bigger size, the lower porosity affected the rate to some extent. The corroborative evidence comes from the results of the experiment no.11 where the big pellet had a higher porosity compared to the big pellet of experiment no.26 but the flow rate of CH_4 was lower in the first case. The latter experiment showed an identical reduction rate as shown by the former one though the latter one was carried out at a higher flow rate. Therefore, it could be possible that if the pellet (experiment no.26) whose data have been shown in fig.IV.9 had higher porosity it would have exhibited a higher reduction rate and therefore would have approached closer to what is expected for a reaction controlled by gas film diffusion.

From fig.IV.7, apparent activation energies for reduction of Fe_2O_3 by H_2 (equation IV.2) have been obtained as 45 KJ/g.mole and 15.3 KJ/g.mole in the temperature range of $950^\circ\text{C} - 1025^\circ\text{C}$ and $875^\circ\text{C} - 950^\circ\text{C}$ respectively. Apparent activation energy for diffusion in $\text{H}_2 - \text{H}_2\text{O}$ gas mixture has been estimated as 13.4 KJ/g.mole⁽²⁶⁾. This is another proof that the reaction is controlled by diffusion through gas boundary layer, particularly at lower temperatures. Probability of controlling by interfacial chemical reaction at higher temperature is unlikely because control by chemical reaction at higher temperature and the control by diffusion through gas film at lower temperature is not possible. Moreover, for the reaction being controlled by interfacial chemical reaction, F vs. t curves should be drooping in nature which has not been observed. One possible explanation for high apparent activation energy at higher temperatures can be as follows.

The gas phase in the present system was a multicomponent mixture consisting of CH_4 , H_2 , H_2O etc. As the temperature increases, the concentration of CH_4 decreases and that of H_2 increases appreciably. As the methane molecules are much heavier than the hydrogen molecules, the apparent interdiffusion coefficient for counterdiffusion of H_2 and H_2O is expected to increase much more than in the simple $\text{H}_2 - \text{H}_2\text{O}$ gas mixture as the temperature is raised. This indicates the possibility of higher apparent activation energy even

though the reduction is controlled by diffusion through gas boundary layer. Quantitative estimates could not be presented because of the complicated calculation procedure for diffusion in multicomponent gas mixture.

So, in brief, it can be stated that the decomposition of CH_4 which takes place mainly on the Mullite furnace tube into C and H_2 (equation no.IV.1) controls the overall rate primarily. However diffusion through the gas film seems to control the actual reduction reaction (equation no.IV.2).

The above interpretation is a qualitative one. It does not seem to be possible to assert more positively. As such iron oxide reduction is a complex phenomenon owing to various structural factors like porosity of the pellet, pore size, change of pore size with temperature, size change of pellet on reduction, topochemical or non-topochemical pattern of reduction, presence of several phases during the progress of reduction etc.etc. Moreover, more than one rate controlling step have been encountered in many cases. So, for a simple system like reduction of Fe_2O_3 by H_2 there are many investigations with many complexities and controversies^(27,28). The present investigation deals with a much more complex system due to the presence of various reactions as well as due to the effect of multicomponent diffusion. Moreover, carbon deposition on pellet, pellet swelling etc. have made the situation more complicated. Therefore, it is neither possible nor desirable to try to interpret more rigorously.

IV.11 Comparison with Literature :

Let the fraction of CH_4 being decomposed into H_2 in blank experiment be x . So, 1 mole of inlet CH_4 gas produces $(1-x)+2x$ i.e. $1+x$ moles of exit gas. Therefore, mole fraction of H_2 in the exit gas (X_{H_2}) = $\frac{2x}{1+x}$. In other words, $x = \frac{X_{\text{H}_2}}{2-X_{\text{H}_2}}$.

The table IV.4 presents the variation of x with temperature in the blank experiments at approximately steady state condition.

Table IV.4 Variation of x with temp.

<u>Experiment No.</u>	<u>Temperature($^{\circ}\text{K}$)</u>	<u>x</u>
21	1298	0.361
14	1223	0.159
16	1148	0.053

Plot of $\log x$ vs. $\frac{1}{T}$ (Fig.IV.10) from the above data yields an activation energy of 163.8 KJ/g.mole. This is much less than what is reported in literature^(29, 7). According to Laidler⁽²⁹⁾, the activation energy for decomposition of CH_4 is 423 KJ/g.mole whereas Eisenberg and Bliss⁽⁷⁾ have reported this value as 355 KJ/g.mole. ~~This lower value may be due to catalytic effect of reduced iron as has been shown by~~ However, Misra⁽⁵⁾, ~~It has been reported there~~ that the activation energy for decomposition of CH_4 on reduced iron was 63.84 KJ/g.mole which is far less than what is reported by Laidler or Eisenberg et al. ~~Another~~ ^{The} reason for lowering of activation energy value

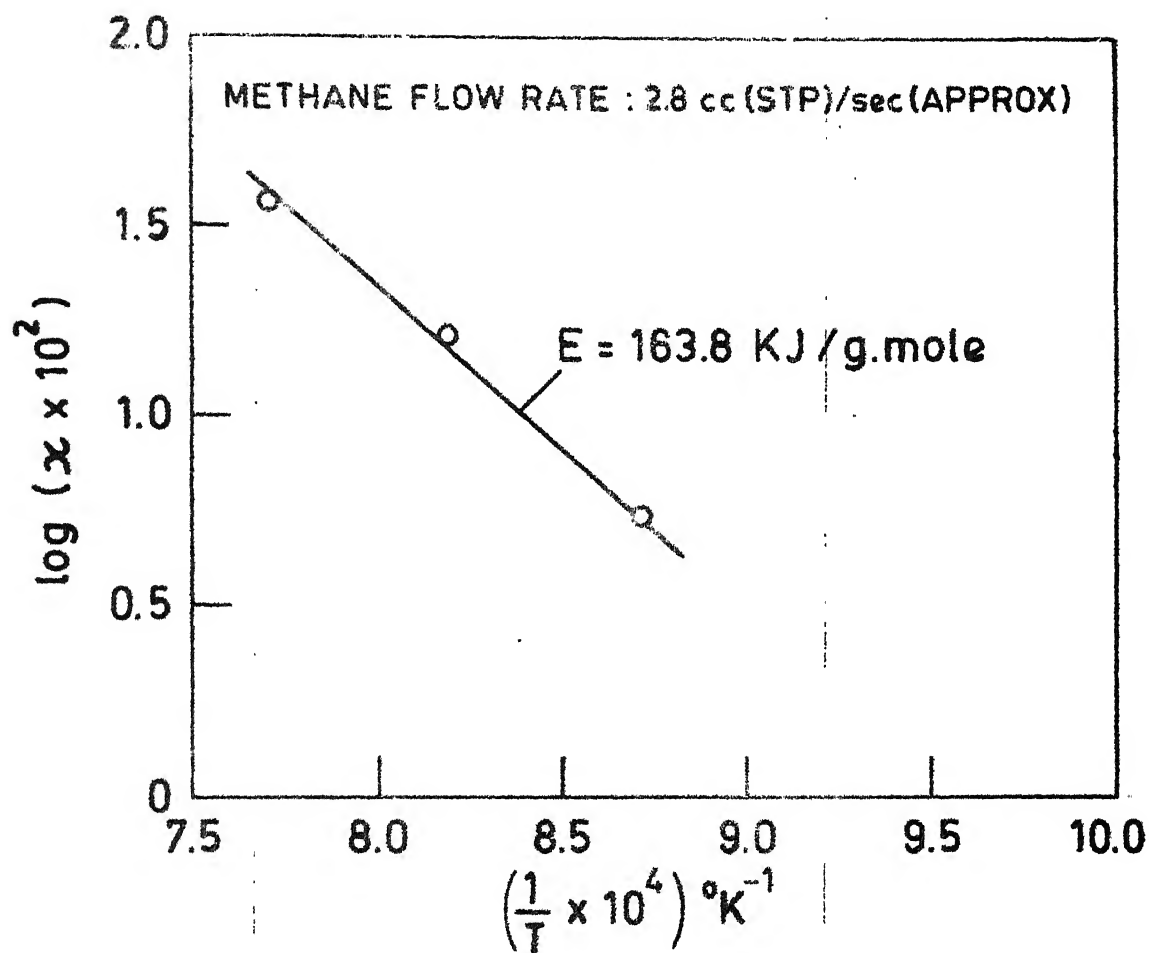


FIG. IV.10 - ARRHENIUS - TYPE PLOT FOR METHANE DECOMPOSITION IN BLANK EXPERIMENTS.

in the present case may be slow heating and slow cooling of gas which was not the case in other investigations. Assuming the constant temperature zone in the present investigation of length 8 cm., residence time of gas at hot zone at 1025°C was calculated as 12 seconds. Extrapolating data from Eisenberg et al., it is seen that this much conversion should have taken place in 3.5 seconds only. So, the difference in the activation energy value can be partially attributed to slow heating as well as slow cooling of the gas in the present system, which tend to lower the effective temperature in the hot zone of the furnace.

At higher flow rate the effective temperature of the gas in the hot zone is expected to be even less. This effect actually might lower the concentration of H_2 in the gas at higher flow rate, thereby decreasing the rate of reduction. Misra⁽⁵⁾ used much higher flow rates (12 cc/sec.) in his experiments. He found lower rates of reduction as compared to the present investigation. It is likely that the effect discussed above might have caused this discrepancy.

All these discussions point out that the reduction by CH_4 would perhaps be slower by factor of 20 or more as compared to H_2 reduction if Mullite furnace tube did not help in the decomposition of CH_4 . However, nothing more can be stated about it at this stage.

CHAPTER -V

SUMMARY AND CONCLUSIONS

1. The experimental set-up consisting of three major units, viz. methane generation and storage, gas train, and thermogravimetric set-up were designed and fabricated to study the reducibility of iron oxide in methane-containing gases.
2. Altogether 30 experiments were carried out. Most of them were reduction experiments. H_2 , CH_4 , $H_2 + CH_4$ and CH_4 followed by H_2 were used as reducing gases for the reduction of spherical Fe_2O_3 pellets at four different temperatures like $800^\circ C$, $875^\circ C$, $950^\circ C$ and $1025^\circ C$. Exit gas was analysed along with the measurement of fractional reduction (F) of the pellet. Carbon deposition on the pellet due to cracking of CH_4 was also measured in many experiments.
3. Decomposition of CH_4 into C and H_2 took place mostly on the Mullite furnace tube inside which the pellet was hung.
4. The results with CH_4 as reducing gas showed a reproducible tendency of F vs. t curves to be linear after a certain period. On an average this steady state varied from $F \approx 0.3$ to $F \approx 0.9$.
5. The rates of reduction by CH_4 were approximately lower by a factor of 5 at $950^\circ C$ in comparison to that by H_2 . The lower rate of reduction with CH_4 , could not be explained either by pore blockage due to deposited carbon or by

'reagent starvation effect' which was proved to be insignificant. However, it has been justified by the lower partial pressure of hydrogen during CH_4 reduction.

6. Reduction rate increased with increase in temperature, methane flow rate and pellet size. Dense pellets ($\epsilon \approx 0.05$) exhibited a greater rate of oxygen removal compared to porous pellets ($\epsilon \approx 0.3$).

7. Carbon deposition on pellet increased with increase in temperature. Carbon was found to penetrate inside the pellet.

Reduced pellet showed an increase in size at all temperatures, except at 1025°C , when pure CH_4 was the reducing gas. This was a contrast to what had happened during reduction with pure H_2 .

The experiment, with the purpose of pellet temperature measurement, recorded a substantial drop in temperature inside the pellet.

8. The reduction of Fe_2O_3 was a two stage process. Decomposition of CH_4 into C and H_2 was followed by the reduction of Fe_2O_3 by H_2 .

At both $F = 0.2$ and $F = 0.7$, apparent activation energy of the overall reduction process was found to be around 210 KJ/g.mole in the temperature range of $800^\circ\text{C} - 950^\circ\text{C}$ and as 105.7 KJ/g.mole in the temperature range of $950^\circ\text{C} - 1025^\circ\text{C}$.

For the actual reduction step (i.e. reduction of iron oxide by H_2), at $F = 0.7$, the apparent activation energy was obtained as 15.3 KJ/g.mole in the temperature range of $875^\circ C - 950^\circ C$ and as 45.0 KJ/g.mole in the temperature range of $950^\circ C - 1025^\circ C$. The activation energy for the decomposition of CH_4 in the present system was obtained as 163.8 KJ/g.mole.

9. Decomposition of CH_4 was found to primarily control the over-all reduction rate. However, diffusion through the gas boundary layer seemed to control the actual reduction reaction i.e. reaction of Fe_2O_3 with H_2 .

CHAPTER VI

RECOMMENDATIONS FOR FURTHER WORK

Very few investigations have been done over this problem. The present one can be taken as a preliminary work. Lot of investigations can be done in this field depending on the objective. Therefore, no concrete recommendation for further work would be made.

R E F E R E N C E S

1. W.A. Mullett, I.G. Nixon, and J.D. Smith, J. Iron Steel Inst., 211 (1973), 278 - 283.
2. I.G. Nixon, Ironmaking Steelmaking, 1 (1980), 2 - 12.
3. I.G. Nixon, Paper presented at Inst. Chem. Engg. Symp., Series No. 43, Harrogate, 1975, 13 - 7f.
4. I.G. Nixon, C.F. Simpson, and J.D. Smith, Ironmaking Steelmaking, 2 (1976), 106 - 107.
5. A.K. Misra, M.Tech. Thesis, I.I.Sc., Bangalore (1976).
6. G. Egloff, R.E. Schaad, and C.D. Lowry, J. Phys. Chem., 34 (1930), 1617 - 1740.
7. B. Eisenberg, and H. Bliss, 'Recent Advances in Kinetics', Chem. Engg. Progress Symp. Series, 63 (1967), 1.
8. Syskov, and Jelikhovastya, Carbon, 5 (1967), 201.
9. T.J. Hirt, and H.B. Palmer, Carbon, 1 (1963), 65.
10. L.F. Albright and C.F. McConnell, 175th ACS National Meeting, March 12 - 17 (1978).
11. H.M. Stanley and A.W. Nash, J. Soc. Chem. Ind, 48 (1929) 1T.
12. R.V. Wheeler and W.L. Wood, Fuel, 7 (1928), 535.
13. A.I. Vogel, 'Text Book of Quantitative Inorganic Analysis', 468 - 472.
14. Handbook of Chemistry and Physics, 43rd. Edition.
15. B. Rama Devi, Internal Report, Met. Engg. Deptt., I.I.T., Kanpur.
16. S.N. Basu, and A. Ghosh, J. Iron Steel Inst., August (1970), 765 - 769.
17. S.N. Basu, M. Tech. Thesis, I.I.T., Kanpur (1968).

18. W.M. Mckewan, Trans. Met. Soc. AIME, 218 (1960), 2-6.
19. J.F. Elliott, and M. Gleiser, Thermochemistry for Steelmaking, 1.
20. L.S. Darken, and E.T. Turkdogan, 'Adsorption and Kinetics at Elevated Temperatures'. Heterogeneous Kinetics at Elevated Temperatures (G.R. Belton, W. L. Worrel, Tds), Plenum Press, Now York (1970), 25.
21. P.L. Walker, Jr., M. Shelef, and R.A. Anderson, 'Catalysis of Carbon Gasification'. Chemistry and Physics of Carbon (P.L. Walker Ed.), Marcel Dekker, Inc., New York 4 (1968), 287.
22. Y.K. Rao, Met. Trans. AIME, 2 (1971), 149.
23. R.N. Singh, and A. Ghosh, Indian J.Tech., 6 (1968), 334.
24. F.S. Mannin and W.O. Philbrook, 'Rate Phenomena', Ch.17 ' ' Blast Furnace Theory and Practice ' ' (Julius H. Strassburger Ed.), Gordon and Breach, New York, (1969);
25. S. Fillinov, ' 'The Theory of Metallurgical Processes' ', 161.
26. R.G. Olsson and W.M. Mckewan, Trans. Met. Soc. AIME, 236 (1966), 1518.
27. R.H. Spitzer, F.S. Manning, and W.O. Philbrook, Trans. Met. Soc. AIME, 236 (1966), 1715.
28. E.T. Turkdogan and J.V. Vinters, Met. Trans., 2 (1971), 3175.
29. K.J. Laidler, ' ' Chemical Kinetics ' ', 396.

A P P E N D I X

Appendix A.I : Experimental ResultsExperiment No.1

Pellet Weight (W) = 0.890gm., Pellet Diameter (d_o) = 0.775cm.,
 Fractional Porosity of Pellet (ϵ) = 0.306,
 Temperature (T) = 1073 °K,
 Volumetric Flow Rate of Inlet Gas (\dot{V}) = 13.6cc(STP)/sec., H_2
 Flushing Gas : $N_2(\phi)$.

<u>Time(secs.)</u>	<u>Fractional Reduction(F)</u>	<u>Gas Analysis</u>	<u>Observations/ Comments, if any</u>
180	0.499	Not done	Slight crack on reduced pellet surf- ace was seen
300	0.839		
420	0.988		
540	1.000		

... (ϕ) Flushing gas would be Argon, if not mentioned
 otherwise, in the following experiments.

Experiment No.2

W = 0.875 gm., d_o = 0.758 cm., ϵ = 0.271, T = 1073°K,
 \dot{V} = 14.8 cc (STP)/sec., H_2 , Flushing Gas : N_2

<u>Time(secs.)</u>	<u>F</u>	<u>Gas Analysis</u>	<u>Comments</u>
60	0.211	Not done	-
120	0.405		
240	0.744		
360	0.917		
480	0.937		
600	0.995		

Experiment No.3

$W = 2.298 \text{ gm.}, \quad d_0 = 0.963 \text{ cm.}, \quad \epsilon = 0.067, \quad T = 1073 \text{ }^\circ\text{K},$
 $\dot{V} = 15.00 \text{ cc(STP)/sec.}, \text{ H}_2.$

<u>Time(secs.)</u>	<u>F</u>	<u>Gas Analysis</u>	<u>Comments</u>
60	0.034		
180	0.113		
300	0.191		
540	0.345		
900	0.538	Not done	-
1260	0.698		
1800	0.878		
2160	0.946		
2700	0.980		

Experiment No.4

$W = 0.930 \text{ gm.}, \quad d_0 = 0.802 \text{ cm.}, \quad \epsilon = 0.346, \quad T = 1223 \text{ }^\circ\text{K},$
 $\dot{V} = 18.24 \text{ cc(STP)/sec.}, \text{ H}_2.$

<u>Time(secs.)</u>	<u>F</u>	<u>Gas Analysis</u>	<u>Comments</u>
60	0.289		
120	0.609		
180	0.826		
240	0.924	Not done	-
360	0.996		
540	1.000		

Experiment No.5

$W = 1.834 \text{ gm.}, \quad d_o = 0.866 \text{ cm.}, \quad \epsilon = 0.000, \quad T = 1223^\circ\text{K},$
 $\dot{V} = 18.24 \text{ cc(STP)/sec.}, \quad \text{H}_2.$

No Realistic Data Was Obtained as The Pellet Cracked
 Too Much (Almost Powdered).

Experiment No.6

$W = 1.204 \text{ gm.}, \quad d_o = 0.843 \text{ cm.}, \quad \epsilon = 0.271, \quad T = 1223^\circ\text{K},$
 $\dot{V} = 0.75 \text{ cc(STP)/sec.}, \quad \text{CH}_4.$

<u>Time(secs.)</u>	<u>F(ϕ)</u>	<u>Gas Analysis (Mole Fraction)</u>			<u>Comments</u>
		H ₂	CH ₄	Ar(Balance)	
60	0.053				
240	0.192				
300		0.02	0.056		
480	0.305				Gas ana- lysis was not much re- liable.
720	0.358				
900	0.429				
1200	0.546				
1440	0.651				
1500		0.36	0.36		
1860	0.847				
2100	0.956				

(ϕ) Hence forth, F would represent apparent fractional reduction of the pellet as it could not exclude carbon deposition on the pellet. However, in the plots F stands for actual fractional reduction which has been obtained from these data; by taking maximum F (0.956 in this case) as 1.000. It can be noted that difference between apparent fractional reduction and actual fractional reduction was very small.

Experiment No.7

$W = 1.186 \text{ cm.}, \quad d_o = 0.830 \text{ cm.}, \quad \epsilon = 0.246, \quad T = 1223 \text{ }^\circ\text{K},$
 $\dot{V} = 0.75 \text{ cc(STP)/sec.}, \quad \text{CH}_4.$

<u>Time(secs.)</u>	<u>F</u>	<u>Gas Analysis</u>	<u>Comments</u>
90	0.107		
270	0.256		
510	0.306		
690	0.394		This expt. was meant for Repro- ducibility checking of expt. no.6.
930	0.463	Not done	
1170	0.585		
1410	0.681		
1710	0.925		
1950	0.960		

Experiment No.8

$W = 2.261 \text{ cm.}, \quad d_o = 0.959 \text{ cm.}, \quad \epsilon = 0.070, \quad T = 1223 \text{ }^\circ\text{K},$
 $\dot{V} = 0.75 \text{ cc(STP)/sec.}, \quad \text{CH}_4.$

<u>Time(secs.)</u>	<u>F</u>	<u>Gas Analysis(Mole Fraction)</u>			<u>Comments</u>
		<u>H₂</u>	<u>CH₄</u>	<u>Ar(Balance)</u>	
60	0.066				
360	0.224	0.16	0.39		
720	0.323	0.26	0.49		
1020	0.387				
1320	0.469	0.28	0.52		
2100	0.664	0.31	0.46		
2880	0.846	0.34	0.48		
3540	0.962				

Experiment No.9

$W = 1.258 \text{ gm.}, d_0 = 0.857 \text{ cm.}, \epsilon = 0.275, T = 1223^\circ \text{K},$

$\dot{V} = 0.75 \text{ cc(STP)/sec.}, \text{CH}_4$: First 6 Minutes

$14.75 \text{ cc(STP)/sec.}, \text{H}_2$: Rest of the Period.

<u>Time(secs.)</u>	<u>F</u>	<u>Gas Analysis</u>	<u>Comments</u>
60	0.047		
120	0.130		
240	0.234		
360	0.285		
CH ₄ stopped and H ₂ passed		Not done	-
420	0.339		
480	0.533		
600	0.825		
720	0.965		
840	0.966		
900	0.973		

Experiments No.10

$W = 1.211 \text{ gm.}, d_0 = 0.837 \text{ cm.}, \epsilon = 0.251, T = 1223^\circ \text{K},$

$\dot{V} = 0.75 \text{ cc(STP)/sec.}, \text{CH}_4$: First 21 Minutes

$15.00 \text{ cc(STP)/sec.}, \text{H}_2$: Rest of the Period.

<u>Time(secs.)</u>	<u>F</u>	<u>Gas Analysis</u>	<u>Comments</u>
60	0.037		
120	0.097		
360	0.262		
600	0.341		
840	0.423	Not done	-
1260	0.588		
CH ₄ stopped and H ₂ passed			
1380	0.752		
1440	0.854		
1530	0.962		
1620	0.985		

Experiment No.11

$W = 4.258 \text{ g.}, d_0 = 1266 \text{ cm.}, \epsilon = 0.238, T = 1223^\circ \text{K},$

$\dot{V} = 1.5 \text{ cc(STP)/sec.}, \text{CH}_4$

Time(secs.)	F	Gas Analysis(Mole Fraction)			Observation
		H ₂	CH ₄	Ar(Balance)	
60	0.008	0.003	0.06		
300	0.089				
600	0.207	0.15	0.44		Slight crack on pellet surface.
960	0.305	0.22	0.57		
1200	0.350	0.25	0.51		
1800	0.479	0.32	0.65		
2700	0.702	0.31	0.57		
3720	0.995				

Experiment No.12

$W = 1.213 \text{ g.}, d_0 = 0.865 \text{ cm.}, \epsilon = 0.321, T = 1148^\circ \text{K},$

$\dot{V} = 0.75 \text{ cc(STP)/sec.}, \text{CH}_4, \text{ Flushing Gas : N}_2$

Time(secs.)	F	Gas Analysis(Mole Fraction)				Observation
		N ₂	CH ₄	CO ₂	H ₂ (Balance)	
60	0.011					
240	0.048	0.55	0.47	-		
600	0.133	0.32	0.56	0.03		
1200	0.254					
1800	0.309	0.10	0.64	0.06		-
3000	0.379					
2280	0.332	0.07	0.69	0.05		
4500	0.497					
6000	0.656					
7200	0.792					
8220	0.976					

Experiment No.13

W = 1.273 gm., $d_0 = 0.883$ cm., $\epsilon = 0.328$, $T = 1073$ °K,
 $\dot{V} = 0.75$ cc(STP)/sec., CH_4 .

Time(secs.)	F	Gas Analysis(Mole Fraction)			Observation
		H_2	CH_4	Ar(Balance)	
60	0.004				
240	0.007	0.003	0.09		
900	0.028	0.009	0.38		
1500	0.053	0.010	0.76		
2100	0.071	0.017	0.86		
2700	0.089	0.018	0.97		
3300	0.114	0.02	0.99		
5400	0.174	0.03	0.99		
6000	0.192	0.03	0.99		
7500	0.242 ϕ				

ϕ After this, experiment was deliberately stopped by switching CH_4 off.

Experiment No.14

W = 1.245 gm., $d_0 = 0.873$ cm., $\epsilon = 0.321$, $T = 1223$ °K,
 $\dot{V} = 2.77$ cc(STP)/sec., CH_4 .

Time(secs.)	F	Gas Analysis(Mole Fraction)			Observation
		H_2	CH_4	Ar(Balance)	
60	0.054				
420	0.330	0.20	0.62		
780	0.570	0.27	0.60		
1140	0.778	0.29	0.60		
1320	0.875	0.28	0.59		
1500	0.954	0.30	0.58		
1560	0.961				

Slight crack on pellet surface.

Experiment No.15

$W = 1.178 \text{ gm.}, \quad d_0 = 0.848 \text{ cm.}, \quad \varepsilon = 0.299, \quad T = 1223^\circ \text{K},$
 $\dot{V} = 2.76 \text{ cc(STP)/sec.}$

Time(secs.)	F	Gas Analysis(Mole Fraction)			Comments/ Observation
		H ₂	CH ₄	Ar(Balance)	
60	0.008				
240	0.188	0.04	0.10		(i) This experiment was meant for reproducibility checking of expt. no.14
480	0.357	0.15	0.55		
660	0.481	0.17	0.60		
780	0.545	0.19	0.61		
1020	0.713				
1380	0.978	0.27	0.60		(ii) Slight crack on pellet surface.
1440	0.986				

Experiment No.16

$W = 1.244 \text{ gm.}, \quad d_0 = 0.849 \text{ cm.}, \quad \varepsilon = 0.264, \quad T = 1148^\circ \text{K},$
 $\dot{V} = 2.62 \text{ cc(STP)/sec.}$

Time(secs.)	F	Gas Analysis(Mole Fraction)				Observation
		CH ₄	Ar	CO ₂	H ₂ (Balance)	
120	0.025	0.33	0.64	-		
360	0.090	0.70	0.27	0.02		
600	0.154	0.84	0.13	0.02		
1080	0.262	0.89	0.03	0.02		
1680	0.341	0.98	0.01	-		-
2280	0.416	0.98	0.01	-		
3600	0.607	0.97	0.01	-		
4800	0.786	0.94	0.01	-		
6000	0.977					

Experiment No.17

W = 2.174 gm., $d_o = 0.939$ cm., $\epsilon = 0.046$, $T = 1223$ °K,
 $\dot{V} = 2.84$ cc(STP)/sec., CH_4 .

Time(secs.)	F	Gas Analysis(Mole Fraction)				Observation
		CH_4	Ar	CO_2	H_2 (Balance)	
120	0.037					
240	0.084	0.56	0.16	0.01		(i) Reduction itself stopped unusually after F=0.802.
480	0.147	0.61	0.05	-		
720	0.266					
1080	0.471	0.67	0.02	-		
1320	0.602					
1560	0.708	0.62	0.01	-		(ii) Reduced pellet showed deformation of its surface.
1920	0.802					

Experiment No.18

W = 1.238 gm., $d_o = 0.868$ cm., $\epsilon = 0.313$, $T = 1223$ °K,

$\dot{V} = 2.77$ cc(STP)/sec., CH_4 : First 11 Minutes
 14.82 cc(STP)/sec., H_2 : Rest of the Period,

Flushing Gas : N_2 .

Time(secs.)	F	Gas Analysis(Mole Fraction)			Observation
		H ₂	CH ₄	N ₂ (Balance)	
60	0.007	0.006	0.10		
180	0.104	0.06	0.37		
300	0.219				
480	0.316	Not Ca-0.70			
660	0.421	lculat-			
CH ₄ stopped and H ₂ passed					
720		Not Ca-0.05			
900	0.881	lculat-			
1080	0.978	1.0	-		

Experiment No.19

$W = 1.291 \text{ gm.}, d_o = 0.876 \text{ cm.}, \epsilon = 0.304, T = 1223^\circ \text{K},$

$\dot{V} = 2.32 \text{ cc(STP)/sec.}, \text{CH}_4$

+

$7.65 \text{ cc(STP)/sec.}, \text{H}_2$.

Time(secs.)	F	Gas Analysis(Mole Fraction)			Observation
		CH_4	H_2	Ar(Balance)	
120	0.342				
240	0.622	0.16	0.59		
480	0.942	0.18	0.69		Crack on the redu- ced pell- et surfa- ce.
600	0.975	0.16	0.69		
660	0.978				

Experiment No.20

$W = 1.211 \text{ gm.}, d_o = 0.838 \text{ cm.}, \epsilon = 0.253, T = 1073^\circ \text{K},$

$\dot{V} = 2.77 \text{ cc(STP)/sec.}, \text{CH}_4$.

Time(secs.)	F	Gas Analysis(Mole Fraction)			Observation
		H_2	CH_4	Ar(Balance)	
60	0.015	0.006	0.66		
480	0.031	0.009	0.81		
960	0.054	0.01	0.91		
1440	0.085	0.01	0.99		
1920	0.112	0.01	0.98		
2880	0.170				
3600	0.201	0.015	0.985		
4320	0.229 ^φ				

φ After this, experiment was stopped by switching CH_4 off.

Experiment No.21

W = 1.217 gm., $d_o = 0.873$ cm., $\epsilon = 0.337$, $T = 1298$ °K,
 $\dot{V} = 2.70$ cc(STP)/sec., CH_4 .

Time(secs.)	F	Gas Analysis(Mole Fraction)			Observation
		H_2	CH_4	Ar(Balance)	
60	0.015				(i) CH_4 flow rate was little unsteady.
120	0.096	0.11	0.13		
300	0.359	0.34	0.28		
540	0.683	0.42	0.36		(ii) CH_4 cracked too much.
660	0.849				(iii) In chromatograph, one gas (possibly CO) component appeared, in between H_2 and CH_4 , in very small amounts.
780	0.930	0.51	0.38		
900	0.968				

Experiment No. 22

W = 1.236 gm., $d_o = 0.873$ cm., $\epsilon = 0.326$, $T = 1298$ °K,
 $\dot{V} = 2.77$ cc(STP)/sec., CH_4 .

<u>Time (secs.)</u>	<u>F</u>	<u>Gas Analysis</u>	<u>Observation/Comments</u>
60	0.019		
120	0.057		(i) This expt. was meant for Reproducibility checking of expt.no.21
300	0.327		
540	0.657	Not done	
660	0.817		(ii) Observations are same as in expt.no.21.
780	0.938		
900	0.969		

Experiment No. 23

This was a 'Blank Experiment' (i.e. experiment without pellet).

$$T = 1223^{\circ}\text{K}, \quad \dot{V} = 2.78 \text{ cc(STP)/sec.}, \quad \text{CH}_4.$$

Time(secs.)	Gas Analysis(Mole Fraction)			Comments
	<u>H₂</u>	<u>CH₄</u>	<u>Ar(Balance)</u>	
300	0.04	0.33		This expt. was carried out to analyse the exit gas, in absence of the pellet at 950°C.
480	0.17	0.52		
600	0.22	0.60		
990	0.26	0.63		
1200	0.27	0.64		

Experiment No. 24

$$W = 1.206 \text{ gm.}, \quad d_o = 0.852 \text{ cm.}, \quad \epsilon = 0.292, \quad T = 1298^{\circ}\text{K}, \\ \dot{V} = 2.70 \text{ cc(STP)/sec.}, \quad \text{CH}_4.$$

This experiment was performed to determine extent of carbon deposition on the pellet at $F \simeq 0.4$ (Carbon-determination Result in Table III.1). So, Gas Analysis and Reduction data were not collected.

Experiment No.25

$W = 1.244 \text{ gm.}, \quad d_o = 0.865 \text{ cm.}, \quad \epsilon = 0.303, \quad T = 1298^\circ \text{K},$
 $\dot{V} = 3.23 \text{ cc(STP)/sec.}, \quad \text{CH}_4.$

This experiment was performed to determine the extent of carbon deposition on the pellet, at $F \geq 0.7$ (Carbon-determination Result in Table III.1). So, Gas Analysis and Reduction data were not collected.

Experiment No.26

$W = 3.578 \text{ gm.}, \quad d_o = 1.15 \text{ cm.}, \quad \epsilon = 0.146, \quad T = 1223^\circ \text{K},$
 $\dot{V} = 2.77 \text{ cc(STP)/sec.}, \quad \text{CH}_4.$

Time(secs.)	F	Gas Analysis(Mole Fraction)			Comments
		Ar	CH ₄	H ₂ (Balance)	
60	0.019	0.78	0.22		The desired ϵ of the pellet was 0.30 approx. But unfortunately it could not be achieved.
960	0.301				
1560	0.442				
2160	0.602				
2760	0.764	0.03	0.60		
3120	0.846	0.02	0.54		
3480	0.922	0.02	0.57		
3840	0.956	0.02	0.59		

Experiment No.29

This was a 'Blank Experiment' (i.e. experiment without any pellet)

$$T = 1298^{\circ}\text{K}, \quad \dot{V} = 2.78 \text{ cc(STP)/sec.}, \quad \text{CH}_4.$$

Time(secs.)	Gas Analysis(Mole Fraction)			Comments
	H ₂	CH ₄	Ar(Balance)	
120	0.27	0.17		This experiment was carried out to analyse the exit gas in absence of pellet at 1025°C.
300	0.47	0.33		
540	0.53	0.39		
720	0.57	0.41		
900	0.55	0.45		
1020	0.61	0.40		

Experiment No.30

This was a 'Blank Experiment' (i.e. experiment without any pellet).

$$T = 1148^{\circ}\text{K}, \quad \dot{V} = 2.77 \text{ cc(STP)/sec.}$$

Time(secs.)	Gas Analysis(Mole Fraction)			Comments
	H ₂	CH ₄	Ar(Balance)	
120	0.09	0.34		This experiment was carried out to analyse the exit gas in absence of pellet at 875°C.
360	0.09	0.57		
720	0.12	0.77		
1080	0.13	0.80		
1260	0.10	0.77		

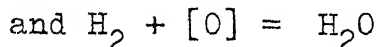
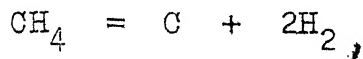
Appendix A.IIProcedure for (p_{H_2O}/p_{H_2}) Actual Calculation(i) For Intermediate and Later Periods :

Let \dot{V} be the volumetric flow rate (cc(STP)/sec.) of CH_4 and y be the fraction of CH_4 which has been decomposed to produce C and H_2 at a particular time at which $(p_{H_2O}/p_{H_2})_{\text{actual}}$ is to be calculated and at which gas analysis also is known.

Some of the above H_2 reacts with Fe_2O_3 to give H_2O .

Let \dot{W}_O be the rate of oxygen removal in gm/sec. which can be obtained from the reduction data.

Let us consider the following two reactions,



where $[O]$ is the oxygen of Fe_2O_3 .

Assumptions : It is assumed that H_2O does not react elsewhere. Also, formation of CO , CO_2 etc. by auxiliary reactions are considered negligible.

Calculations : Rate of oxygen removal from $Fe_2O_3 = \dot{W}_O$ gm.
 $= \frac{\dot{W}_O}{16}$ gm. atoms.

∴ no. of moles of H_2 which react with $[O] = \frac{\dot{W}_O}{16}$ (to produce $\frac{\dot{W}_O}{16}$ moles of H_2O).

Out of $\frac{\dot{V}}{22400}$ moles of CH_4 , $\frac{\dot{V}y}{22400}$ moles have been decomposed to produce $\frac{2\dot{V}y}{22400}$ moles of H_2 .

Let us now prepare a table of inlet and exit gases :

<u>Inlet</u>	<u>Exit</u>
$\text{CH}_4 : \frac{\dot{V}}{22400} \text{ moles}$	$\text{CH}_4 : \left(\frac{\dot{V}}{22400} - \frac{\dot{V}y}{22400} \right) \text{ moles}$
	$\text{H}_2 : \left(\frac{2\dot{V}y}{22400} - \frac{\dot{W}_0}{16} \right) \text{ moles}$
	$\text{H}_2\text{O} : \frac{\dot{W}_0}{16} \text{ moles}$

From the above,

$$\frac{p_{\text{CH}_4}}{p_{\text{H}_2}} = \frac{\dot{V}(1-y)}{2\dot{V}y - 1400\dot{W}_0}$$

From gas analysis data L.H.S. is known. \dot{V} and \dot{W}_0 being known, y can be obtained.

$$\text{As, } \left(\frac{p_{\text{H}_2\text{O}}}{p_{\text{H}_2}} \right)_{\text{Actual}} = \frac{1400 \dot{W}_0}{2\dot{V}y - 1400 \dot{W}_0},$$

The L.H.S. can be obtained as everything in R.H.S. are known.

(ii) For Initial Periods :

Let, fraction of CH_4 being decomposed by z (assuming negligible H_2O formation). Let us consider 1 mole of CH_4 as inlet gas.

<u>Inlet</u>	<u>Exit</u>
1 mole CH_4	$(1-z)$ mole CH_4
	2z mole H_2

$$\text{So, } \frac{X_{\text{CH}_4}}{X_{\text{H}_2}} = \frac{1 - z}{2z}$$

L.H.S. is known from gas analysis. So, \hat{z} can be obtained.

Let \dot{V}_{inlet} be the volumetric flow rate of CH_4 in the inlet. Due to the abundance of flushing gas inside the furnace during initial periods, working flow rate of CH_4 (\dot{V}) will be less than \dot{V}_{inlet} .

As 1 mole of CH_4 produces $(1+z)$ moles of exit gases, \dot{V} volume of CH_4 should produce $\dot{V} (1+z)$ cc(STP) of exit gas per sec.

$$\text{So, } \dot{V} (1+z) = \dot{V}_{\text{exit}} (X_{\text{CH}_4} + X_{\text{H}_2})$$

$$\text{Assuming, } \dot{V}_{\text{exit}} = \dot{V}_{\text{inlet}}$$

$$\therefore = \frac{\dot{V}_{\text{inlet}} (X_{\text{CH}_4} + X_{\text{H}_2})}{\dot{V}}$$

$$\dot{V} = \frac{\dot{V}_{\text{inlet}} (X_{\text{CH}_4} + X_{\text{H}_2})}{1 + z}$$

Now, as in case of intermediate and later period,

$$\frac{X_{\text{CH}_4}}{X_{\text{H}_2}} = \frac{\dot{V} (1 - y)}{2\dot{V}y - 1400 \dot{W}_0}$$

where, y = fraction of CH_4 cracked
(taking care of H_2O formation)

$$\text{and } \left(\frac{p_{\text{H}_2\text{O}}}{p_{\text{H}_2}} \right)_{\text{Actual}} = \frac{1400 \dot{W}_0}{2\dot{V}y - 1400 \dot{W}_0}$$

As, R.H.S. terms are already known, $(p_{\text{H}_2\text{O}}/p_{\text{H}_2})_{\text{Actual}}$ value can be obtained.

A 65988

This book is to be returned on the
date last stamped.

This image shows a blank sheet of white paper with horizontal blue ruling lines. A single vertical red margin line runs down the center of the page, creating two equal-width columns. The lines are evenly spaced and extend across the entire width and height of the page.

CD 6.72.9

ME-1981-M-GHO-RED